Molecular Therapy
Nucleic Acids
Original Article

IL-10 modified mRNA monotherapy prolongs survival after composite facial allografting through the induction of mixed chimerism

Ana Elena Aviña,[1,2] Dante De Paz,[1,3,4] Shu-Chun Huang,[5,6,7] Kuan-Hung Chen,[6,7] Yun-Ching Chang,[8,9] Chin-Ming Lee,[1] Chia-Hsien Lin,[1] Fu-Chan Wei,[1,3,7] and Aline Yen Ling Wang[1]

[1]Center for Vascularized Composite Allotransplantation, Chang Gung Memorial Hospital, Taoyuan 333, Taiwan; [2]Clinical Fellow, Department of Plastic and Reconstructive Surgery, Chang Gung Memorial Hospital; Chang Gung University and Medical College, Taoyuan 333, Taiwan; [3]Department of Plastic Surgery, Chang Gung Memorial Hospital, Taoyuan 333, Taiwan; [4]Department of Head and Neck Surgery, National Police Hospital, Lima 15072, Peru; [5]Department of Physical Medicine and Rehabilitation, New Taipei Municipal Tucheng Hospital, Chang Gung Memorial Hospital, New Taipei 236, Taiwan; [6]Department of Physical Medicine & Rehabilitation, Chang Gung Memorial Hospital, Taoyuan 333, Taiwan; [7]College of Medicine, Chang Gung University, Taoyuan 333, Taiwan; [8]Department of Health Industry Technology Management, Chung Shan Medical University, Taichung 402, Taiwan; [9]Department of Medical Research, Chung Shan Medical University Hospital, Taichung 402, Taiwan

Vascularized composite allotransplantation has great potential in face transplantation by supporting functional restoration following tissue grafting. However, the need for lifelong administration of immunosuppressive drugs still limits its wide use. Modified mRNA (modRNA) technology provides an efficient and safe method to directly produce protein *in vivo*. Nevertheless, the use of IL-10 modRNA-based protein replacement, which exhibits anti-inflammatory properties, has not been shown to prolong composite facial allograft survival. In this study, IL-10 modRNA was demonstrated to produce functional IL-10 protein *in vitro*, which inhibited pro-inflammatory cytokines and *in vivo* formation of an anti-inflammatory environments. We found that without any immunosuppression, C57BL/6J mice with fully major histocompatibility complex (MHC)-mismatched facial allografts and local injection of IL-10 modRNA had a significantly prolonged survival rate. Decreased lymphocyte infiltration and pro-inflammatory T helper 1 subsets and increased anti-inflammatory regulatory T cells (Tregs) were seen in IL-10 modRNA-treated mice. Moreover, IL-10 modRNA induced multilineage chimerism, especially the development of donor Treg chimerism, which protected allografts from destruction because of recipient alloimmunity. These results support the use of monotherapy based on immunomodulatory IL-10 cytokines encoded by modRNA, which inhibit acute rejection and prolong allograft survival through the induction of donor Treg chimerism.

INTRODUCTION

Vascularized composite allotransplantation (VCA) is an emerging form of treatment in the field of surgical reconstruction.[1–4] It is particularly useful in cases in which a defect is too large or unique to repair using conventional methods. Most defects caused by tumor resection, trauma, and reconstruction of congenital anomalies can be repaired using autologous tissues. However, unique defects in areas such as the face, hand, uterus, penis, etc., can only be replaced through VCA.[5–19] VCA differs from solid organ transplantation in that it uses a composite of tissue types. Taking the face, for example, an allograft would contain various tissue components, such as skin, muscle, mandible, oral mucosa, vessels, and nerves, which have various levels of immunogenicity.[20–22] Compared with organ transplantation, VCA elicits complicated and aggressive immune rejection responses.[23] Therefore, patients need lifelong immunosuppression and are at risk for opportunistic infections or tumor formations. If the dose of immunosuppressive drugs can be reduced, perhaps VCA could be more available to the patients who need it most.

Interleukin-10 (IL-10) has an important function in the maintenance of immune balance. It suppresses alloantigen presentation of antigen-presenting cells (APCs) and renders these cells more tolerogenic.[24–27] IL-10 also inhibits the expression of pro-inflammatory cytokines such as IL-2, IL-1β, tumor necrosis factor-α (TNF-α), and interferon-γ (IFN-γ).[28–33] Anti-inflammatory regulatory T cells (Tregs) can be differentiated from naive T cells by IL-10 treatment,[34] which mainly contributes to immunosuppression[35] and inhibits various pro-inflammatory cells.[36] Donor corneas pre-treated with transforming growth factor β and IL-10 recombinant proteins displayed prolonged allograft survival through the induction of tolerogenic APCs.[37] IL-10 gene therapy was performed using intramuscular injection of adeno-associated virus (AAV), which resulted in suppression of diabetes recurrence when diabetic mice were transplanted with islet cells. Moreover, the serum level of IL-10 was positively correlated with

Received 8 July 2022; accepted 11 February 2023;
https://doi.org/10.1016/j.omtn.2023.02.016.

Correspondence: Aline Yen Ling Wang, Center for Vascularized Composite Allotransplantation, Chang Gung Memorial Hospital, Taoyuan 333, Taiwan.
E-mail: aline2355@yahoo.com.tw

extended islet graft survival, whereas it was negatively associated with diabetic autoimmune responses.[38] Skeletal muscle transduction with AAV-IL-10 effectively prevents spontaneous type 1 diabetes and inhibits insulin autoantibodies and insulitis in nonobese diabetic (NOD) mice.[39] Intramuscular injections of IL-10 plasmid DNA also prevent spontaneous diabetes in NOD mice.[40] Taking all the data together, IL-10 administrations shown to protect against islet destruction by suppressing autoimmunity through the use of IL-10 recombinant protein therapy (subcutaneous, intramuscular, or oral injection) or gene therapy (AAV or plasmid administration). In contrast, several studies reported that IL-10 administrations are highly associated with the severity of graft-versus-host disease (GVHD).[41–43] IL-10 infusion has a dose-dependent effect on GVHD lethality through the modulation of $CD4^+$ and $CD8^+$ T cells. High doses of IL-10 administration exacerbate GVHD lethality, whereas low doses of IL-10 mediate protection for GVHD.[42]

Compared with therapy based on protein or DNA, mRNA has several advantages, such as rapid production of the target protein, low purification cost, easy operation, and lack of genomic integration. However, there are disadvantages, such as instability, immunogenicity, and difficult delivery, which limit the therapeutic application of mRNA. In recent years, scientists have substantially overcome the disadvantages of mRNA therapy with modified mRNA (modRNA) technology using anti-reverse cap analog (ARCA), 5-methylcytidine-5′-triphosphate, pseudouridine-5′-triphosphate, and other modifications. It was demonstrated that ARCA does not interact with reverse oriented mRNA, resulting in increased mRNA stability and translation efficiency.[44,45] The incorporation of modified nucleotides such as 5-methylcytidine (5mC) and pseudouridine (ψU) and a poly-A tail was reported to enhance mRNA stability and decrease innate immune responses in the host.[46] Phosphatase also facilitates reduced host immunity by the removal of triphosphates at the 5′ end of the mRNA. Therefore, modRNA can mediate highly transient expression and has low immunogenicity, and its stability is enhanced, as it avoids degradation by RNase enzymes. modRNA is a safe, effective, and footprint-free strategy with a half-life of up to 6 days *in vivo*.[47] Studies have demonstrated that following intracardiac injection, purified vascular endothelial growth factor (VEGF) modRNA can immediately produce VEGF protein in heart tissue and further improve heart function.[47–50] A single injection of dendritic cells (DCs) electroporated with IL-4 modRNA was shown to prevent autoimmune diabetes and maintain stable glycemia in nonobese diabetic mice through the upregulation of Tregs.[51] Moreover, modRNA technology has also been used for various purposes in clinical trials of several diseases, including in targeting VEGF in cardiovascular disease, tumor-specific antigen in prostate cancer, and vaccine in human immunodeficiency virus.[52] modRNA-based vaccines against coronavirus disease 2019 (COVID-19), such as Pfizer/BNT 162b2 using proline mutations and Moderna 1273 using N1-methyl-pseudourine, are widely available worldwide.[53–57]

However, the effects of IL-10 modRNA monotherapy in composite facial allotransplantation have not yet been studied. We used modRNA with local injection to directly produce IL-10 protein around the facial allograft *in vivo* and subsequently evaluated allograft survival and the underlying mechanisms. We hypothesized that the transient overexpression of anti-inflammatory cytokine IL-10 protein has an important immunomodulatory role in the process of donor Treg induction and acute allograft rejection.

RESULTS

Protein produced from IL-10 modRNA transcript is functional *in vitro*

To distinguish between endogenously and exogenously expressed IL-10, our construct was cloned with a FLAG tag in the C terminus of IL-10 gene. Gene sequence corresponding to either IL-10 or IL-10_FLAG was separately cloned into an RNA synthesis vector using the Gibson Assembly method for *in vitro* transcription. DNA sequencing and gel electrophoresis were used in the characterization of both constructs, the latter of which was used to visualize the PCR transcript and EcoRI-cut fragments (Figure S1). To confirm whether the purified IL-10 modRNA transcript translates a protein that is actually secreted, we used several cell lines for transfection, including mouse embryonic fibroblasts (MEFs), C2C12 mouse muscle myoblasts, human embryonic kidney 293 cells, and human Jurkat T cells. GFP modRNA was used as a positive control to evaluate the transfection efficiency of modRNA in these cells. GFP protein expression was detected 6 h after transfection, with robust expression levels observed in the cells at 24 and 48 h post-transfection by fluorescence microscopy (Figure S2). On the basis of quantitative ELISA, different cell types were all similarly found to secrete increased IL-10 protein in a time-dependent manner after modRNA transfection (Figures 1A–1D). The expression of IL-10 protein from modRNA transcript in Jurkat cells was examined using qualitative western blot assay (Figure 1E). A Transwell system was used to evaluate whether the protein secreted from IL-10 modRNA-transfected Jurkat cells was functional, namely whether it could inhibit pro-inflammatory cytokines such as IL-2 and IFN-γ produced from stimulated mouse splenocytes. We found that the IL-10 modRNA group showed a time-dependent and quantitative decrease in IL-2 and IFN-γ production compared with the buffer group (Figures 1F and 1G). These results demonstrate that IL-10 protein is translated from purified modRNA transcript in different cell types, and the secreted protein is functional in inhibiting IL-2 and IFN-γ production in activated lymphocytes.

Tracking of kinetics of the protein produced from luciferase modRNA using *in vivo* image system

Although a cationic lipid is typically used in modRNA encapsulation for *in vivo* delivery,[58] it is associated with significant toxicity issues.[59] Recent studies reported that modRNA can be translated in *in vivo* tissues without the need for lipid carriers.[50] The delivery of modRNA embedded with a transfection reagent, such as RNAiMAX or Lipofectamine, into animal heart tissue *in vivo* was demonstrated to have lower protein expression compared with injection with naked modRNA in a sucrose-citrate buffer.[48] To further determine whether injection with naked modRNA in saline buffer is effectively translated into protein in mice, a non-invasive real-time *in vivo* (IVIS) imaging detection system was used for long-term live animal imaging. This system allows

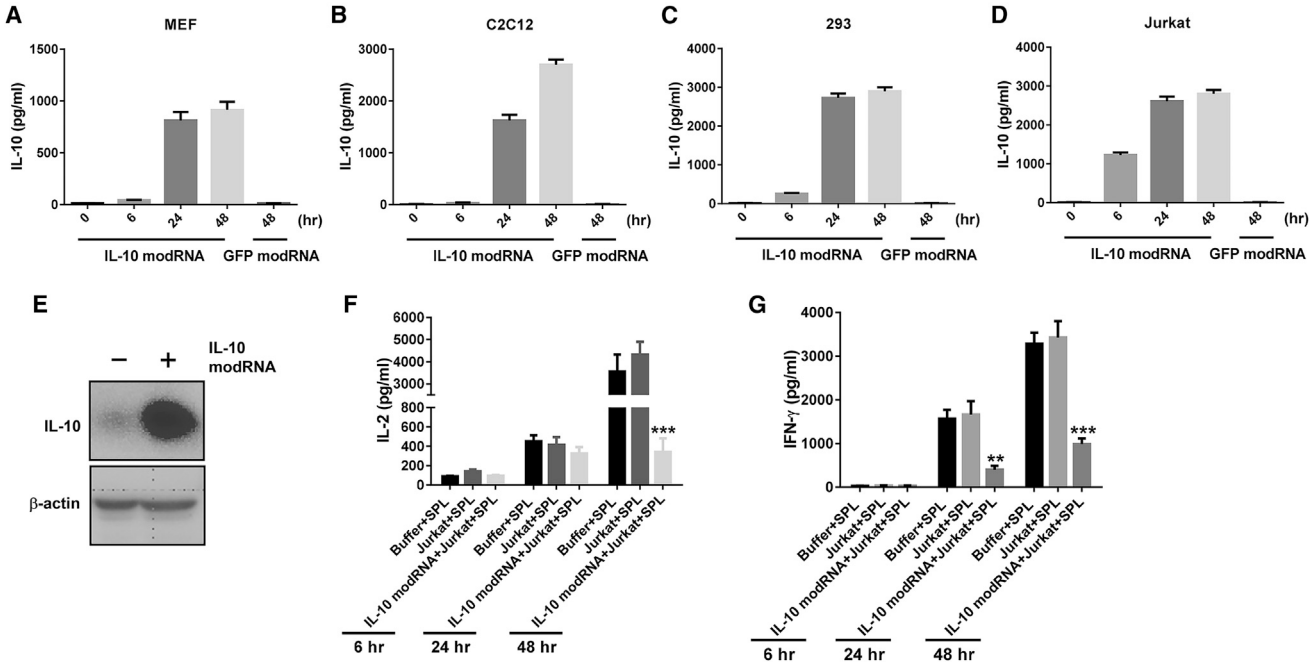

Figure 1. IL-10 modRNA transcript produces functional protein *in vitro*

(A–D) IL-10 modRNA produced IL-10 protein in mouse embryonic fibroblasts (MEFs), C2C12 mouse muscle myoblasts, human embryonic kidney 293 (HEK293) cells, and Jurkat cells (human T cells) at different time points by IL-10 ELISA. MEF (2×10^4), C2C12 (1×10^5), and 293 cells (1×10^5) were transfected with 100 ng modRNA. Jurkat cells (5×10^5) were transfected with 200 ng modRNA. All transfection experiments were performed in 96-well flat plate using Lipofectamine 3000 reagent. (E) Jurkat cells expressed IL-10 protein when transfected with IL-10 modRNA. Jurkat cells (12×10^6) were transfected without or with 5,000 ng IL-10 modRNA in 6-well plate. Cells were harvested one day after transfection, and 20 μg protein extract was analyzed using western blot assay. β-Actin was used as loading control. (F and G) Jurkat cells treated with IL-10 modRNA secreted functional IL-10 protein, which inhibited IL-2 and IFN-γ production *in vitro*. Jurkat cells (3×10^5 cells per well) transfected with 200 ng IL-10 modRNA were seeded in the top chambers of Transwell 96-well plates. Splenocytes (SPL; 3×10^5 cells per well) were seeded in bottom reservoir and stimulated with coated anti-CD3 (2 μg/mL) and soluble anti-CD28 (2 μg/mL). Supernatants in bottom reservoir were collected at different time points and analyzed using IL-2 and IFN-γ ELISA. Statistical data are represented as mean ± SD. The IL-10 modRNA group was compared with the buffer group at different time points (**$p < 0.005$ and ***$p < 0.0005$, Student's t test).

instantaneous observation and characterization of the biodistribution and expression time of target proteins in living animals. Firefly luciferase modRNA was constructed into an RNA synthesis vector and checked by DNA sequencing to confirm the length and identity of the 1,653 bp sequence (Figure S3). Subsequently, the naked luciferase modRNA was subcutaneously injected into the right neck of mice, representing luminescent protein only expressed in the local injection site, and bioluminescence measurement persisted up to 6 days (Figure S4). This result suggests that the use of saline buffer alone for modRNA delivery results in good protein expression in mice.

Pharmacokinetics of IL-10 modRNA-translated protein in mice

To examine whether IL-10 modRNA mediates efficient protein translation *in vivo*, exogenous IL-10 protein expression needs to be distinguished from endogenous expression. Thus, purified IL-10_FLAG modRNA was used for detecting exogenous IL-10 protein using FLAG ELISA. Moreover, two dose groups of IL-10_FLAG modRNA were designed for examining expression time of exogenous IL-10 protein *in vivo*. A single 10 μg dose of purified IL-10_FLAG modRNA formulated in 50 μL saline buffer was directly injected into right face tissue at day 0, defined as the IL-10 modRNA-10 group. On the other hand, two 5 μg doses of purified IL-10_FLAG modRNA formulated in 50 μL saline buffer was directly injected into right face tissue at day 0 and day 12, defined as the IL-10 modRNA-5 group. We also explored whether exogenous IL-10 protein is secreted and released to other tissues such as blood, spleen, and lymph nodes (LNs), in addition to the injected tissue was determined. In IL-10 modRNA-10 group, on days 1–4 following injection, the concentration of IL-10_FLAG fusion protein was, on average, more than 100 μg/mL, measured from 100 mg of injected tissue in 400 μL lysis buffer by FLAG ELISA. On days 5–6 and 10–18, the protein concentration was below 50 and 10 μg/mL, respectively. However, in IL-10 modRNA-5 group, the first 5 μg dose of IL-10_FLAG modRNA displayed a high concentration of IL-10 protein (55.2 μg/mL) in injected tissues on day 1 and then gradually decreased to 6.02 μg/mL on day 9. The second dose of modRNA showed a second high concentration of IL-10 protein (60.5 μg/mL) in injected tissues on day 13 and, subsequently, gradually reduced to 6.7 μg/mL on day 23 (Figure 2A). The fusion protein was almost undetectable in blood, spleen, and LNs. Immunohistochemistry of the injected tissue on day 2 following IL-10_FLAG modRNA injection showed dramatic expression of IL-10_FLAG fusion protein in muscle tissue, secondarily in epidermis

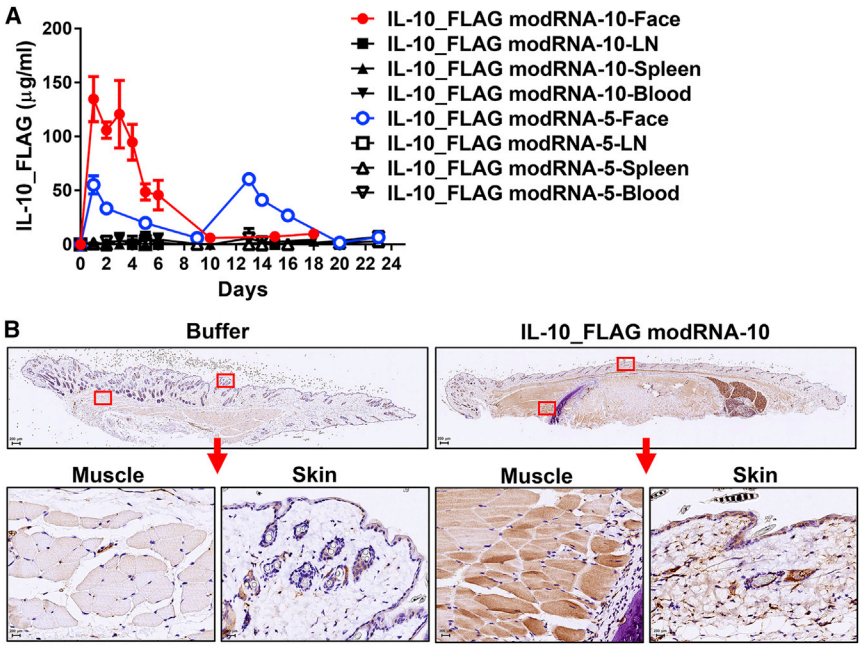

Figure 2. Protein pharmacokinetics in mice injected with IL-10 modRNA

(A) To distinguish between endogenous and exogenous IL-10 expression *in vivo* and further observe the expression time of exogenous IL-10 protein, the IL-10_FLAG modRNA was used, and two dose groups of IL-10_FLAG modRNA were designed in the experiments. A single 10 μg dose of purified IL-10_FLAG modRNA formulated in 50 μL saline buffer was directly injected into right face tissue at day 0, defined as the IL-10 modRNA-10 group. In addition, two 5 μg doses of purified IL-10_FLAG modRNA formulated in 50 μL saline buffer was directly injected into right face tissue at day 0 and day 12, defined as the IL-10 modRNA-5 group. In both groups, blood serum, spleen, lymph nodes (LNs) near injected site, and 100 mg of injected tissue were harvested and analyzed for exogenous IL-10 protein expression using FLAG ELISA. In the IL-10 modRNA-10 group, samples were examined at 0, 1, 2, 3, 4, 5, 6, 10, 15, and 18 days after injection. In the IL-10 modRNA-5 group, samples were examined at 0, 1, 2, 5, 9, 13, 14, 16, 20, and 23 days after injection. Day 0 indicates face tissue without modRNA injection. Harvesting of tissue was conducted using 3 mice for each time point. Data are presented as mean ± SD. (B) Immunohistochemistry of right face tissue on day 2 following injection with saline buffer or 10 μg purified IL-10_FLAG modRNA (IL-10_FLAG modRNA-10 group) at day 0. Scale bars, 200 μm.

and hair follicles, by brown staining of FLAG, which was less brown in connective and fatty tissues (Figure 2B). These results indicate that a single direct injection of naked IL-10 modRNA induces locally transient production for up to 10 days, reaching a peak level at 24 h, corresponding to high translation levels in muscle cells. Although two 5 μg doses of IL-10 modRNA produced around half concentrations of IL-10 protein compared with a single 10 μg dose of modRNA, it can induce locally transient expression for up to 20 days and produce two peak levels on days 1 and 13.

IL-10 modRNA monotherapy prolongs facial allograft survival

The complexity of composite tissues is higher in the face than other body parts, such as the hindlimb, which results in the elicitation of more aggressive immunogenicity, making it difficult to be accepted by the host.[23] Thus, we established a semi-face transplantation mouse model including skin, muscle, oral mucosa, and mandible to study facial VCA therapy and the underlying mechanisms influencing its outcome.[60,61] To explore the effects of IL-10 modRNA-based protein replacement on the acute rejection of facial allograft, semi-faces of BALB/c mice as donors were transplanted to the right necks of C57BL/6J recipient mice without administering immunosuppressive drugs. Moreover, facial transplantation was divided into two groups such as facial osteomyocutaneous (OMC) group with a mandible and myocutaneous (MC) group without a mandible. In the MC group, the mandible was removed from the facial allograft containing skin, muscle, teeth, mandible, oral mucosa, and vessels, while the OMC allograft was a whole hemiface subunit including the mandible. The cuff technique was used to anastomose vessels between the recipient and donor. Representative charts of facial transplantation surgery between both groups are shown in Figures 3A and 3B.

In addition, IL-10 modRNA monotherapy had two groups: a single 10 μg injection of IL-10 modRNA on postoperative day (POD) 3, defined as the IL-10 modRNA-10 group, and two 5 μg injections of IL-10 modRNA on PODs 3 and 15, defined as the IL-10 modRNA-5 group. Saline buffer or IL-10 modRNA diluted in saline was subcutaneously injected with 3 separate injections around the facial allograft. The facial OMC graft was 100% accepted in the syngeneic group using C57BL/6J mice as donors. In facial OMC allotransplantation, rapid invasive necrosis of the facial OMC allograft was seen around PODs 9–12, leading to allograft rejection in the allogeneic buffer group. However, delayed onset and a slow rate of acute rejection were found in facial OMC allografts in the allogeneic group with a single 10 μg dose of IL-10 modRNA. Interestingly, repeat administration of the reduced dose resulted in a further extension of survival for 45 days in the OMC-IL-10 modRNA-5 group. Similar results in facial MC allotransplantation, the IL-10 modRNA-5 group displayed better allograft survival than IL-10 modRNA-10 group, in which both groups significantly prolonged facial MC allografts compared with the MC-buffer group. However, the OMC-buffer, OMC-IL-10 modRNA-10, and OMC-IL-10 modRNA-5 groups exhibited a significantly prolonged survival of facial allografts compared with MC-buffer, MC-IL-10 modRNA-10, and MC-IL-10 modRNA-5 groups, respectively (Figure 3C), suggesting OMC facial allografts have better protection against host alloimmunity than MC allografts. These results demonstrate that repeat administration of the reduced

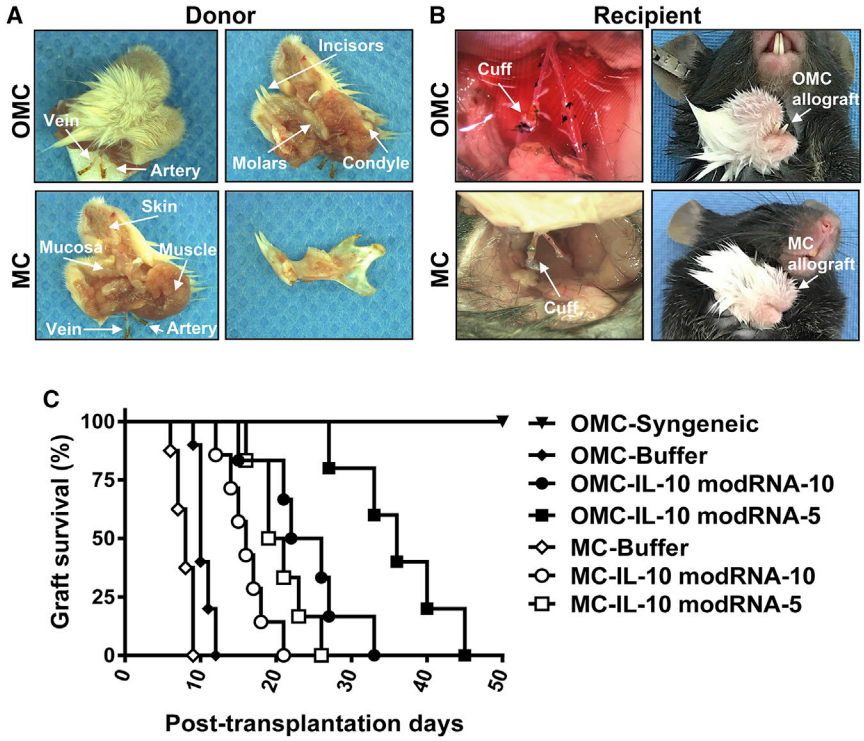

Figure 3. Survival of facial allografts in IL-10 modRNA-treated mice

(A) Donor allograft surgery. The facial osteomyocutaneous (OMC) allograft including mandible, skin, muscle, oral mucosa, and vessels (a whole semi-face subunit), was harvested from a BALB/c mouse. The facial myocutaneous (MC) allograft only containing skin, muscle, oral mucosa, and vessels except for the mandible, was harvested from a BALB/c mouse. (B) Recipient surgery. Harvested allografts were transplanted to the right neck of the recipient C57BL/6J mice by vessel anastomosis using the cuff technique. (C) The impact of IL-10 modRNA monotherapy on facial allograft survival without any immunosuppressive drugs was examined. Fully major histocompatibility complex-incompatible BALB/c facial allografts were grafted onto right necks of C57BL/6J mice. OMC grafts of C57BL/6J mice were used as donors in syngeneic group. OMC-syngeneic, OMC-allogeneic buffer, OMC-allogeneic IL-10 modRNA-10 (single 10 μg dose on POD 3), OMC-allogeneic IL-10 modRNA-5 (two 5 μg doses on PODs 3 and 15), MC-allogeneic buffer, MC-allogeneic IL-10 modRNA-10 (single 10 μg dose on POD 3), and MC-allogeneic IL-10 modRNA-5 (two 5 μg doses on PODs 3 and 15) groups had 8, 10, 6, 5, 8, 7, and 6 mice, respectively. The Kaplan-Meier method was used to calculate facial graft survival. Differences between the three allogeneic groups were significant (OMC-buffer versus OMC-IL-10 modRNA-10, ***p = 0.0002; OMC-buffer versus OMC-IL-10 modRNA-5, **p = 0.0005; OMC-IL-10 modRNA-10 versus OMC-IL-10 modRNA-5, *p = 0.01; MC-buffer versus MC-IL-10 modRNA-10, ***p = 0.0002; MC-buffer versus MC-IL-10 modRNA-5, ***p = 0.0005; MC-IL-10 modRNA-10 versus MC-IL-10 modRNA-5, *p = 0.02; OMC-buffer versus MC-buffer, ****p < 0.0001; OMC-IL-10 modRNA-10 versus MC-IL-10 modRNA-10, **p = 0.0079; OMC-IL-10 modRNA-5 versus MC-IL-10 modRNA-5, **p = 0.0013).

dose (5 μg) of IL-10 modRNA monotherapy significantly prolongs the survival of facial osteomyocutaneous and myocutaneous allografts compared with a single 10 μg dose of modRNA. When facial allografts include mandibles, their survival rates are dramatically enhanced compared with facial allografts without mandibles.

Local injection of IL-10 modRNA decreases lymphocytic infiltration of the facial allograft

To explore the influence of IL-10 modRNA-based protein replacement on facial allograft protection, the levels of lymphocyte infiltration into facial OMC allografts were determined on PODs 10–14. Macroscopic observation showed epidermolysis, diffuse erythema, and necrosis of facial OMC allografts in the buffer group, while soft facial OMC allografts were accepted in allotransplanted mice treated with IL-10 modRNA. Histological H&E staining was used to evaluate the degree of lymphocyte infiltration into facial OMC allografts. Lower levels of lymphocyte infiltration were observed in the IL-10 modRNA group, while there was dramatically enhanced lymphocyte invasion into the dermis, epidermis, and muscle layers of facial OMC allografts, resulting in severe flap damage in the buffer group (Figure 4A). The Banff score showed corresponding results, supporting the levels of lymphocyte infiltration between the two groups. The buffer group presented more severe tissue damage, with the majority of Banff scores being grades III and IV, whereas the IL-10 modRNA group showed major grades I and II (Figure 4A, right).

T cells play a critical role in the elicitation of allograft rejection via activation when recognition of alloantigens, results in allograft damage.[62] To further explore the infiltrated level of T cells in facial OMC allografts between both groups, immunohistochemistry staining was used to observe the infiltrated level of $CD3^+$ T cells and Forkhead box $(FoxP3)^+$ cells into the skin and muscle layers of allografts. Because CD3 is expressed in the cell surface of T cells, the staining displays a circle red. FoxP3 is an important transcription factor and marker for mouse $CD4^+CD25^+$ Tregs and the staining displays a dense red. A single 10 μg dose of IL-10 modRNA displayed a trend toward decreased $CD3^+$ T cells and increased $FoxP3^+$ cells in facial OMC allografts compared with the buffer group (Figure 4B). The quantitation of $CD4^+CD25^+FoxP3^+$ Tregs and $CD3^+$ T cells, including $CD4^+$ and $CD8^+$ T cells, is presented in Figure 6. These results suggest that allotransplanted mice treated with a single local injection of IL-10 modRNA had decreased levels of lymphocyte infiltration, including $CD3^+$ T cells, in favor of $FoxP3^+$ cells into the flap compared with the buffer group, resulting in protection of the facial allograft from rejection.

IL-10 modRNA suppresses inflammation while inducing anti-inflammation

To evaluate the effects of IL-10 modRNA-based protein replacement on alloimmune responses, the production of pro-inflammatory cytokines such as IL-12, IFN-γ, TNF-α, IL-1β, IL-2, and

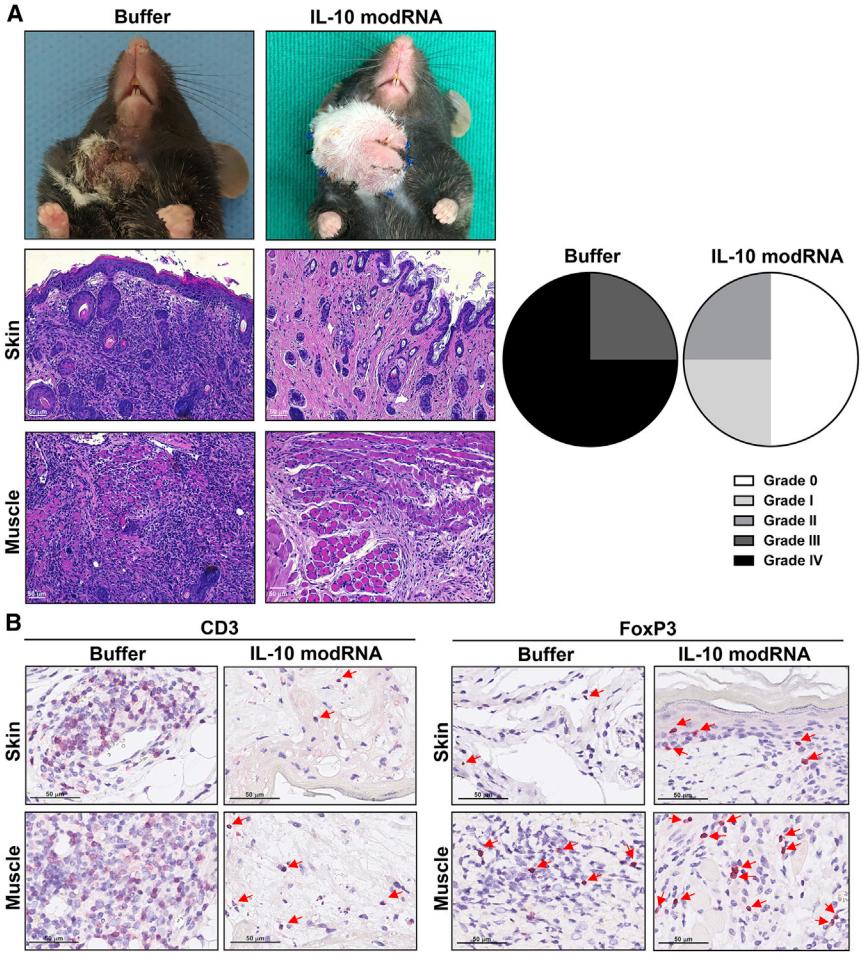

Figure 4. Degree of lymphocytic infiltration into facial allograft

(A) Macroscopic and histological changes (indicated by hematoxylin and eosin staining) in facial OMC allografts of IL-10 modRNA and buffer groups on PODs 10–14. Facial OMC allografts from allotransplanted mice receiving single 10 μg dose of IL-10 modRNA or saline buffer on POD 3 were analyzed. Infiltrating lymphocytes into skin and muscle layers of facial OMC allografts are shown by dense violet staining. Histological Banff classification of facial OMC allografts between buffer and IL-10 modRNA groups is as shown in the right of (A). Each group contains four mice. Scale bars, 50 μm. (B) Immunohistochemistry in facial OMC allografts of IL-10 modRNA and buffer groups on PODs 10–14. Infiltrating $CD3^+$ T cells or $FoxP3^+$ cells into skin and muscle layers of facial OMC allografts are shown by red staining. Because CD3 is expressed in the cell surface of T cells, the staining displays a circle red. FoxP3 is a critical transcription factor and marker for mouse $CD4^+CD25^+$ natural Tregs, and the staining displays a dense red. Scale bars, 50 μm.

IL-17 and anti-inflammatory IL-4 and IL-10 cytokines was analyzed using a Luminex multiplex assay. These cytokines were undetected in the blood serum of both groups (data not shown). IL-12 plays a critical role in the induction of T helper (Th) 1 differentiation from naive $CD4^+$ T cells, which results in the production of pro-inflammatory IFN-γ. In the LNs of IL-10 modRNA group, significantly decreased levels of IL-12 and IFN-γ were observed. In the facial OMC allografts of IL-10 modRNA group, significantly reduced levels of IL-12, TNF-α, and IL-2 were found, whereas a dramatically enhanced level of IL-10 was seen (Figure 5). These results indicate that a single local administration of IL-10 modRNA can suppress inflammation and upregulate anti-inflammatory immune responses in face allotransplantation.

IL-10 modRNA inhibits the development of T helper 1 cells in favor of Treg induction

To study the impacts of IL-10 modRNA-based protein replacement on immune cell populations in face allotransplanted mice, three major subsets of lymphocytes, monocytes, and granulocytes in the blood were first examined on PODs 10–14, which showed similar percentages between the two groups of IL-10 modRNA and buffer (Figure S5). Subsequently, the absolute counts of total immune cells in the blood, spleen, LNs, and facial allograft (allo-face) were calculated in both groups. Although a trend toward reduced absolute counts was observed in blood and spleen, though the difference was not significant. However, in the LNs and facial OMC allografts, total cell numbers were significantly decreased in IL-10 modRNA-treated mice (Figure 6A). The initial activation of T cells and subsequent stimulation of various effector cells resulted in acute rejection.[63,64] APCs such as DCs uptake alloantigen and then present antigen to $CD4^+$ T cells, which contributes to T helper cell activation. Subsequently, these activated cells secrete IFN-γ and TNF-β; IL-2, IL-4, IL-5, and IL-6; and IFN-γ and IL-2 for the activation of macrophages, B cells, and natural killer (NK) cells, respectively. NK cells secrete IFN-γ to mediate innate immunity and granzyme B to directly destroy allografts through cell-mediated cytotoxicity. Macrophages primarily secrete inflammatory mediators of allograft damage. Plasma cells activated from stimulated naive B cells secrete autoantibodies to destroy allograft tissues through antibody-dependent cellular cytotoxicity. To further examine whether IL-10 modRNA-secreted proteins affect the development of different immune cell subsets, flow cytometry was used to analyze $CD4^+$ T, $CD8^+$ T, and $CD19^+$ B cells, $NK1.1^+$ NK cells, $CD11c^+$ DCs, and $CD11b^+$ macrophages. Both buffer and IL-10 modRNA groups displayed similar amounts of these immune cells in blood, spleen, and LNs, and IL-10 modRNA-treated mice showed significantly decreased DC populations in LNs. A trend toward reduced T cells, B cells, DCs, and macrophages was found in the facial OMC allografts of IL-10 modRNA-treated mice compared with the buffer group (Figure 6B).

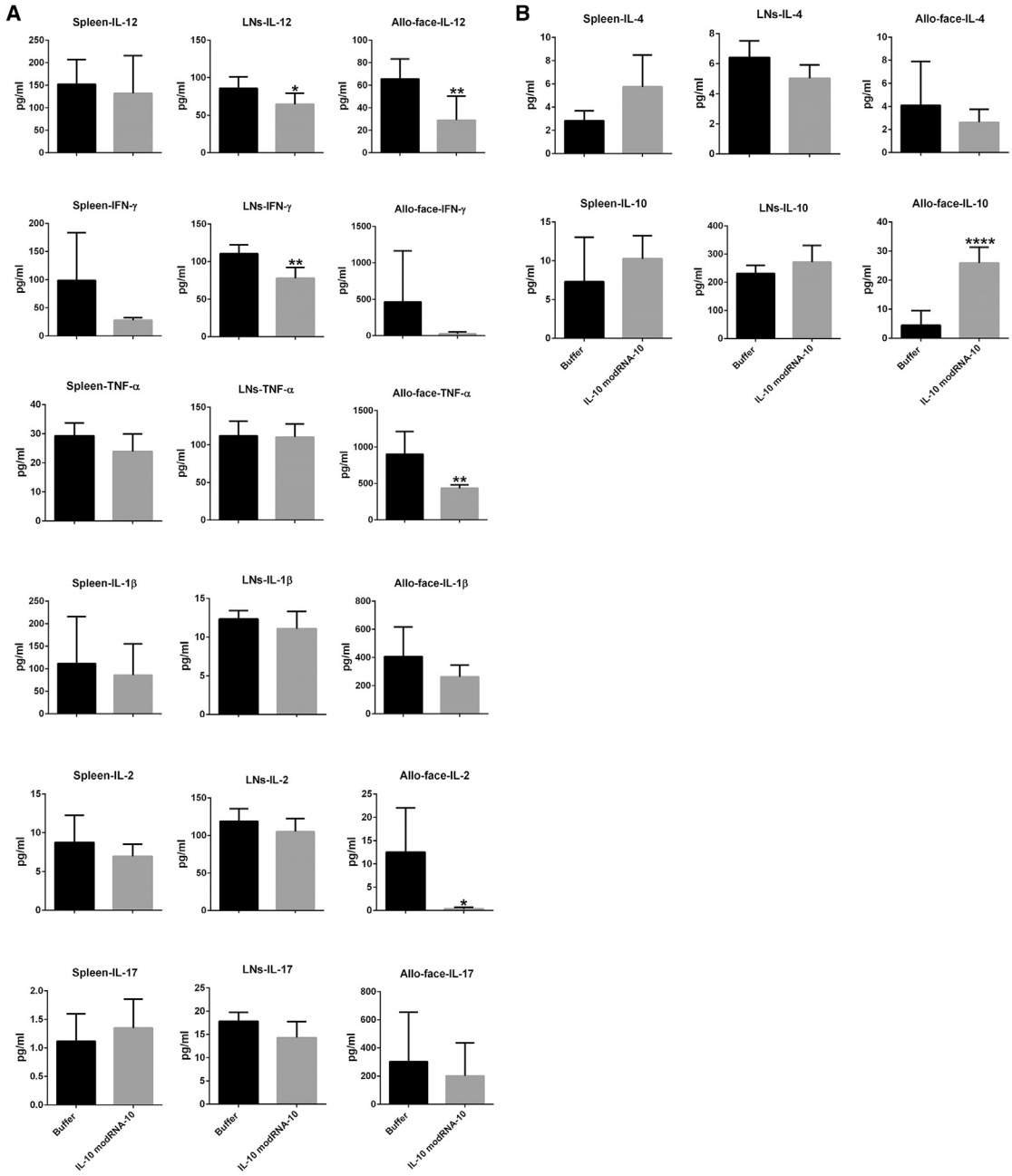

Figure 5. Effects of IL-10 modRNA on the pro-inflammatory and anti-inflammatory cytokine expression in face transplanted mice

Spleen, LNs near OMC allografts, and facial OMC allografts were harvested on PODs 10–14 in buffer and IL-10 modRNA-treated face allotransplanted mice (single 10 μg dose of IL-10 modRNA on POD 3) without any immunosuppressive drugs. (A) The protein levels of pro-inflammatory cytokines such as IL-12, IFN-γ, TNF-α, IL-1β, IL-2, and IL-17 and (B) anti-inflammatory cytokines such as IL-4 and IL-10 were examined using the Luminex multiplex assays in face transplanted mice. Data were collected from three mice in both groups. Statistical data are represented as mean ± SD. The IL-10 modRNA group was compared with the buffer group for lymphoid organs and facial OMC allografts (*$p < 0.05$, **$p < 0.05$, and ****$p < 0.0001$, Student's t test).

As a result of IL-10 modRNA-produced protein in the suppression of inflammatory cytokines in favor of anti-inflammation cytokines, their effects may be through the modulation of different T cell subsets. To further explore the impact of IL-10 modRNA-based protein replacement on the development of different T cell subsets, the populations of pro-inflammatory and anti-inflammatory $CD4^+$ T cells were analyzed using flow cytometry. We determined populations of $CD4^+IFN\text{-}\gamma^+$ Th1 and $CD4^+IL\text{-}17^+$ Th17 cells for

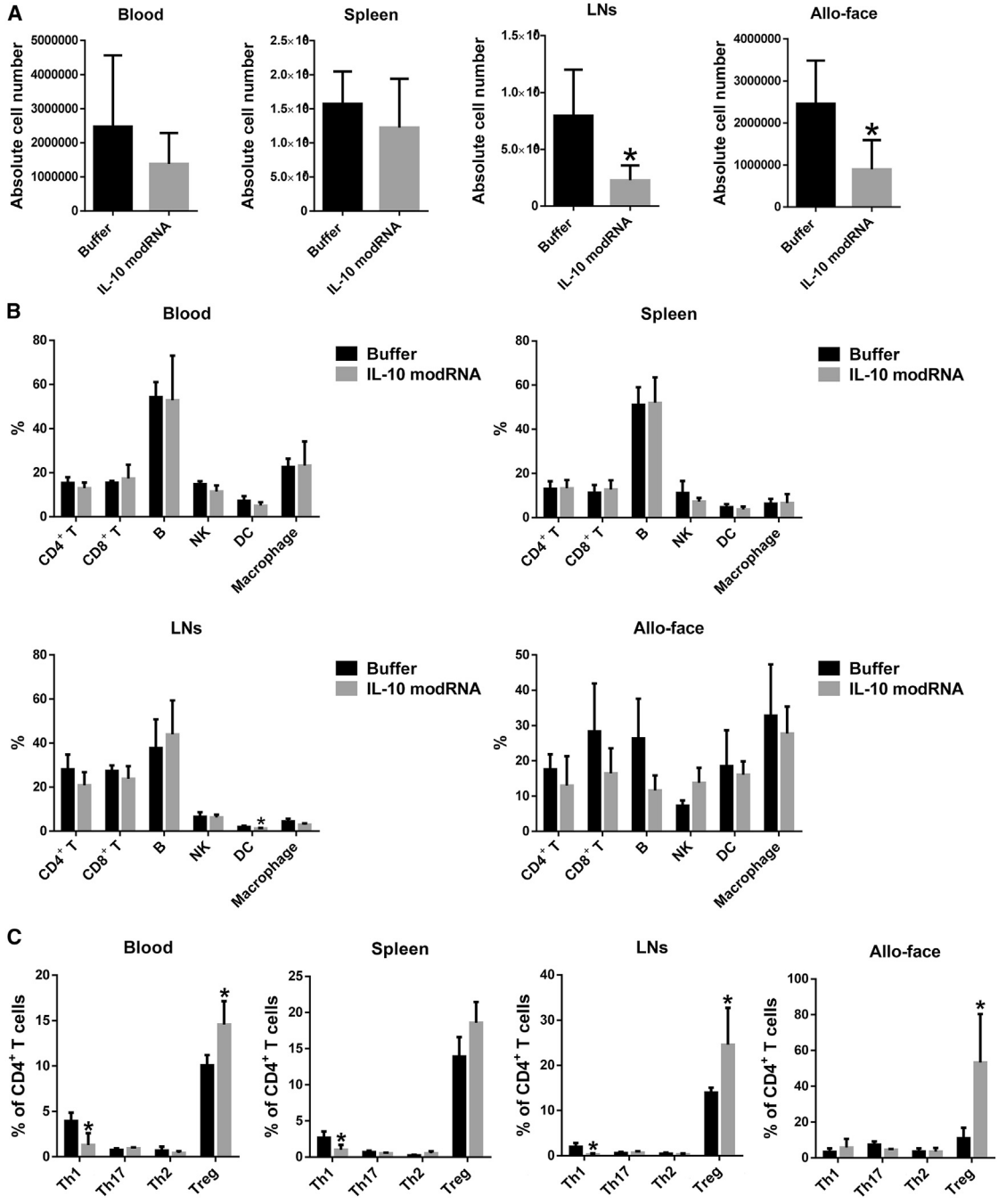

Figure 6. Lymphocyte development in IL-10 modRNA-treated face allotransplanted mice

(A) Absolute cell counts in lymphoid organs and OMC allografts of face allotransplanted mice. White blood cells, spleen, LNs near OMC allografts, and facial OMC allografts were harvested on PODs 10–14 in buffer and IL-10 modRNA-treated face allotransplanted mice (single 10 μg dose of IL-10 modRNA on POD 3) without any immunosuppressive drugs and estimated their absolute cell numbers. (B) Percentages of immune cells in lymphoid organs and OMC allografts of face allotransplanted mice. $CD4^+$ T cells, $CD8^+$ T cells, B cells, NK cells, DCs, and macrophages were stained with anti-mouse CD4-APC, CD8-PE, CD19-APC, NK1.1-PE-Cy7, CD11c-APC, and CD11b-PE, respectively, in different flow tubes to avoid same fluorescence. Percentages of T cells, B cells, and NK cells were gated from lymphocyte population, whereas DCs and macrophages were gated from both lymphocytes and monocytes using flow cytometry. (C) Population of total T helper (Th) 1, Th17, Th2, and regulatory T (Treg) cells in lymphoid organs and OMC allografts of face allotransplanted mice. Pro-inflammatory Th1 and Th17 and anti-inflammatory Th2 and Treg cells were examined using flow cytometry. Th1, Th17, and Th2 cells were surface stained with anti-mouse CD4-APC, and subsequently, they were intracellularly stained with anti-mouse IFN-γ-PerCP,

(legend continued on next page)

assessing pro-inflammatory activity and $CD4^+IL\text{-}4^+$ Th2 and $CD4^+CD25^+FoxP3^+$ Treg cells for anti-inflammatory activity. Both blood and LNs of IL-10 modRNA-treated mice exhibited a significant decrease in Th1 cells and a significant increase in Tregs compared with the buffer group. Spleen showed a major reduction in Th1 cells and a trend toward increased Tregs in the IL-10 modRNA group. Interestingly, in the facial OMC allografts of IL-10 modRNA-treated mice, a dramatically increased percentage of Tregs (53.3%) was found compared with the buffer group (10.8%) (Figure 6C). The percentages of Th17 and Th2 cells were below 1% in the blood, spleen, and LNs of both groups, indicating no significant difference. In facial OMC allografts, a single 10 μg dose of IL-10 modRNA showed a trend toward decreased Th17 cells (4.5%) and increased Th2 cells (10.5%) compared with the buffer group (Th17, 7.3%; Th2, 3.5%), but not significantly. These results indicate that IL-10 modRNA-producing protein suppresses pro-inflammatory Th1 cells and enhances anti-inflammatory total Treg cells in face allotransplanted mice.

IL-10 modRNA monotherapy induces the development of mixed chimerism

Allograft survival has been successfully achieved in mice, swine, nonhuman primates, and humans through the induction of mixed chimerism.[65,66] This refers to the coexistence of donor and recipient immune cells in the host, usually through bone marrow transplantation. Facial OMC allografts that include the mandible have been reported to harbor bone marrow hematopoietic stem cells.[67,68] Our preliminary results demonstrate that the mouse mandible in facial OMC allografts is capable of inducing mixed chimerism in the host,[61] similar to the results showing that the presence of rat mandible in facial allografts is correlated with the induction of chimerism.[69] Therefore, survival following IL-10 modRNA monotherapy-mediated facial allografting without immunosuppressive drugs may be associated with the induction of chimerism. To evaluate the effects of IL-10 modRNA-producing protein on the induction of mixed chimerism, we used flow cytometry to analyze donor immune cells in the host. Because H2d class I histocompatibility antigens are specific to the cells of donor BALB/c mice, we used H2d antibodies to discriminate between donor and recipient cells. Leukocytes were collected and analyzed from lymphoid organs and facial OMC allografts in both groups on PODs 10–14. We found that the percentage of donor immune cells was significantly increased in the blood and LNs, especially in facial OMC allografts (8.8% of buffer versus 21% of IL-10 modRNA) but not in the spleen (Figure 7A).

To further explore whether hematopoietic bone marrow stem cells in the mandible of facial OMC allografts differentiate into donor immune cells, we characterized various donor immune cell subsets, including $CD4^+$ T, $CD8^+$ T, and $CD19^+$ B cells, $NK1.1^+$ NK cells, $CD11c^+$ DCs, and $CD11b^+$ macrophages, using flow cytometry. We found that donor immune cells primarily differentiated into B cells, followed by DCs and macrophages, and then T cells and NK cells in the blood, spleen, and LNs of both groups. The IL-10 modRNA group showed significantly increased T and B cells and macrophages in blood and increased T cells in LNs but not spleen. Especially in facial OMC allografts, dramatic enhancement of NK cells, DCs, and macrophages was observed in the IL-10 modRNA group compared with the buffer group (Figure 7B). These results imply that IL-10 modRNA-producing protein induces mixed chimerism from allo-mandible bone marrow hematopoietic stem cells, leading to multilineage chimerism.

IL-10 modRNA treatment increases donor Treg chimerism

In the facial OMC allografts of IL-10 modRNA-treated mice, a lower percentage of infiltrated lymphocytes (Figure S6) and a higher percentage of donor chimerism were observed. Therefore, we hypothesized a major donor population, such as of Treg cells, mediates protection against the destruction caused by recipient alloimmunity. To test this hypothesis, we examined the population of donor Tregs in the facial OMC allografts of both groups. The marker of donor Tregs was represented as $CD4^+CD25^+FoxP3^+H2Dd^+$, which was first gated from infiltrated lymphocytes, followed by gating of $CD4^+$ T cells, then $CD25^+$ and $FoxP3^+$ Tregs, and finally H-$2Dd^+$ (Figure 8A). Interestingly, the percentage of donor Tregs in IL-10 modRNA-treated mice was significantly increased in the blood and LNs but not the spleen. Especially in facial OMC allografts, the donor Treg population was dramatically enhanced in the IL-10 modRNA group (66.4%) compared with the buffer group (7.5%) (Figure 8B).

As donor Treg chimerism was found to develop from allo-facial mandible hematopoietic bone marrow cells, it was necessary to clarify whether donor Treg cells are homing to the allo-facial (donor) mandible or recruited to the recipient femur, which may provide a special environment to harbor donor Tregs. We found that the percentage of donor immune cells was significantly increased in the donor mandible of facial OMC allografts (12.1% of buffer versus 29.5% of IL-10 modRNA) but not in the recipient femur (Figure S7). Additionally, we further found donor mandible displayed a significantly increased percentage of donor Tregs in the IL-10 modRNA group (59.23%) compared with the buffer group (3.89%). Although the recipient femur showed a trend toward increased donor Tregs in the IL-10 modRNA group (2.83%) compared with the buffer group (0.53%), the difference had no significance (Figure 8C). These results suggest that protein is produced from IL-10 modRNA, which induces the differentiation of donor Tregs and recruits them into facial OMC allografts to form an anti-inflammatory environment, resulting in protection against alloimmunity-mediated destruction. Homing to

IL-17-PE, and IL-4-PE-Cy7, respectively. Additionally, Tregs were surface stained with anti-mouse CD4-APC and CD25-PE, and subsequently, they were intracellularly stained with FoxP3-PerCP. $CD4^+IFN\text{-}\gamma^+$ Th1, $CD4^+IL\text{-}17^+$ Th17, or $CD4^+IL\text{-}4^+$ Th2 cell percentage was analyzed from $CD4^+$ T cells, which were gated from lymphocytes. For the analysis of $CD4^+CD25^+FoxP3^+$Tregs, lymphocytes were gated first, followed by gating of $CD4^+$ T cells, then $CD25^+FoxP3^+$-expressing cells. Buffer and IL-10 groups are black and grey bars, respectively. Data were collected from four mice in both groups. Statistical data are represented as mean ± SD. The IL-10 modRNA group was compared with the buffer group for lymphoid organs and facial OMC allografts (*$p < 0.05$, Student's t test).

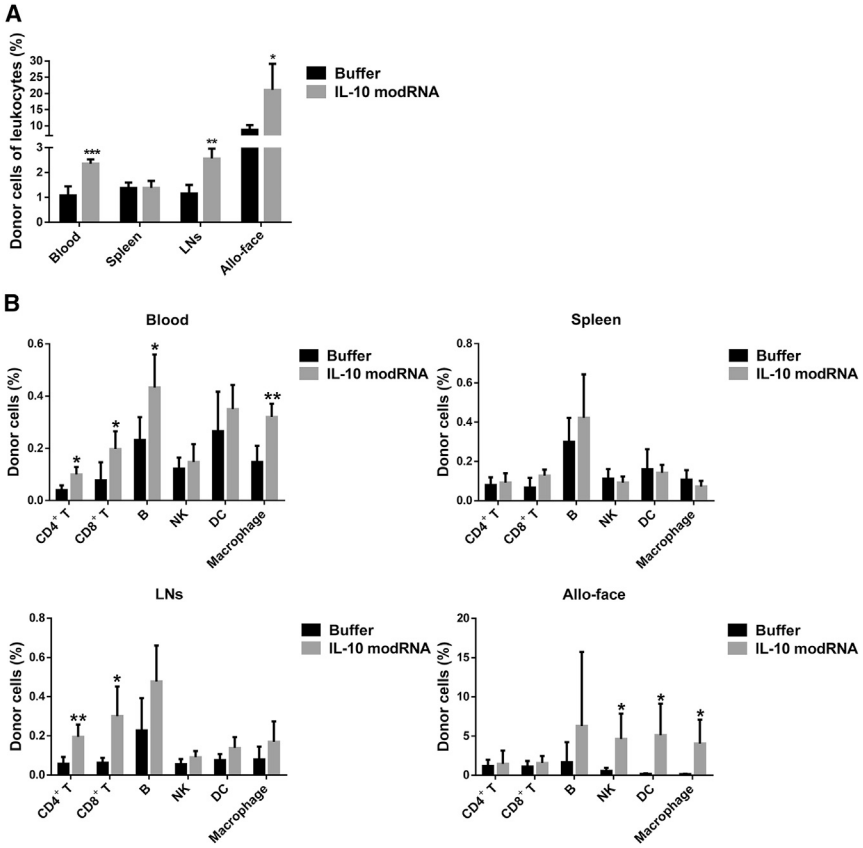

Figure 7. Levels of mixed chimerism in IL-10 modRNA-treated face allotransplanted mice

(A) Effects of IL-10 modRNA-based protein replacement on donor chimerism development. Immune cells were harvested from lymphoid organs and facial OMC allografts from both groups without immunosuppressive drugs on PODs 10–14. Donor immune cells were distinguished by staining anti-mouse H-2Dd-BV421 from recipient cells, which is specific for BALB/c cells. Subsequently, amount of H-2Dd$^+$ donor immune cells in blood, spleen, LNs, and facial OMC allografts was examined using flow cytometry. (B) Impact of IL-10 modRNA-based protein replacement on multilineage chimerism development. Various donor immune cell subsets, including CD4$^+$ T, CD8$^+$ T, B cells, NK cells, DCs, and macrophages, were analyzed and stained with anti-mouse CD4-APC, CD8-PE, CD19-APC, NK1.1-PE-Cy7, CD11c-APC, and CD11b-PE, respectively, and all were further stained with anti-mouse H-2Dd-BV421. Percentages of T cells, B cells, and NK cells were gated from the lymphocyte population and DCs and macrophages were gated from both populations of lymphocytes and monocytes using flow cytometry. Data were collected from four mice in both groups. Statistical data are represented as mean ± SD. IL-10 modRNA group (single 10 μg dose of IL-10 modRNA on POD 3) was compared with the buffer group for lymphoid organs and facial OMC allografts (*$p < 0.05$ and **$p < 0.05$, Student's t test).

and harboring of these donor Tregs in allo-facial mandibles also occurs.

DISCUSSION

In this study, we used the modRNA technique to investigate the relationship of IL-10 protein between the prolongation of facial allograft survival and the induction of mixed chimerism. We demonstrated that IL-10 modRNA transcript can effectively translate secreted IL-10 protein in various cell lines, such as fibroblasts, muscle, kidney cells, and especially T cells. IL-10 protein was demonstrated to be functional in suppressing the production of pro-inflammatory cytokines such as IL-2 and IFN-γ *in vitro*. The saline buffer used as a delivery system formulated with the naked modRNA can induce good expression in mice by the IVIS system, as confirmed by luminescence studies. Moreover, the pharmacokinetics of a single 10 μg dose of naked IL-10 modRNA in mice displayed locally transient production for up to 10 days, peak expression at 24 h, and major translation in the muscle layer of the injected site. Although two 5 μg doses of IL-10 modRNA produced around half concentrations of IL-10 protein compared with a single 10 μg dose of modRNA, it can induce locally transient expression for up to 20 days and produce two peak levels on days 1 and 13. We observed that without any immunosuppression, C57BL/6J mice with fully major histocompatibility complex (MHC)-mismatched facial OMC allografts and one local injection of 10 μg IL-10 modRNA had significantly prolonged survival of 33 days compared with 12 days for control mice without modRNA treatment. Interestingly, face transplanted mice treated with two 5 μg doses of IL-10 modRNA showed a delayed onset and slow rate of acute rejection, resulting in allograft survival of 36 days. IL-10 modRNA monotherapy also displayed protection for facial MC allografts. However, facial allografts include mandibles, and their survival rates are dramatically enhanced compared with facial allografts without mandibles in the presence of IL-10 modRNA or not. Histological H&E staining showed a lower degree of lymphocyte infiltration into the facial allograft and decreased levels of absolute cell numbers for the IL-10 modRNA group, suggesting that the alloimmune responses were modulated. Interestingly, pro-inflammatory Th1 cells were significantly suppressed in the blood, spleen, and LNs, whereas anti-inflammatory Treg cells were dramatically enhanced in the blood, LNs, and facial OMC allografts. This suggests that IL-10 modRNA effectively inhibits inflammation while promoting anti-inflammation as an attempt to balance immune responses in facial composite-elicited alloimmunity. We also found that the level of donor immune cells as an indicator of mixed chimerism was significantly enhanced in blood, LNs, and facial OMC allografts but not spleen. These donor cells even differentiated into various immune cell subsets, a phenomenon referred to as multilineage chimerism. Especially in facial OMC allografts, the donor Treg population was dramatically enhanced compared with the

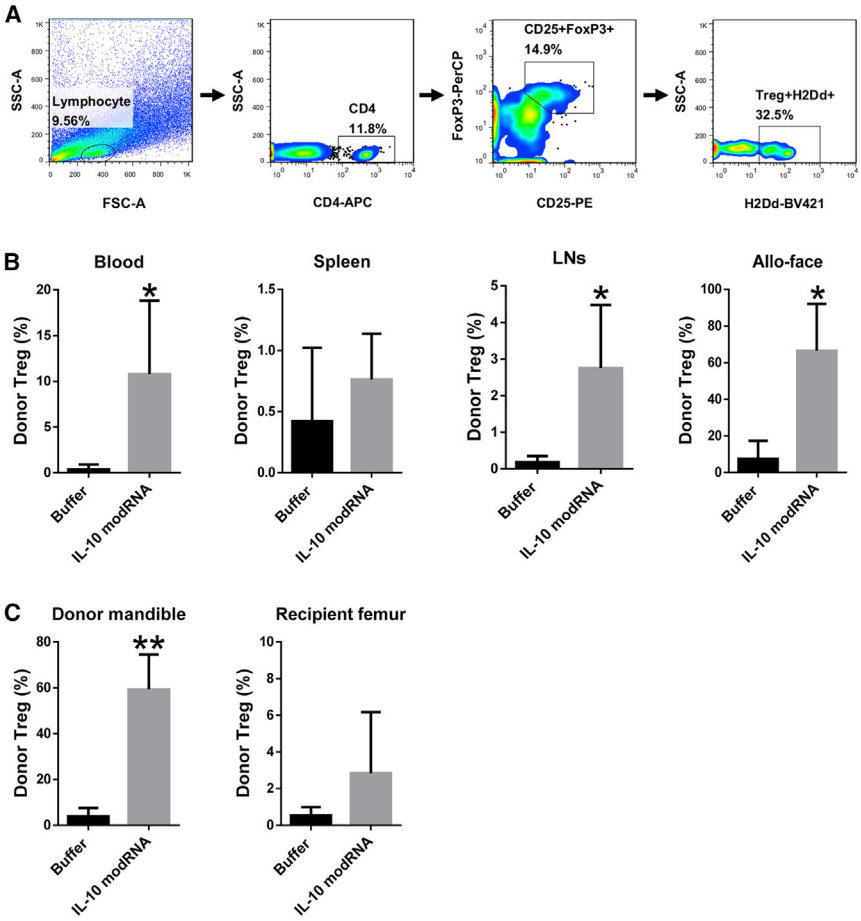

Figure 8. Levels of donor Treg chimerism in IL-10 modRNA-treated face allotransplanted mice

(A) Representation of gating strategy for donor Tregs ($CD4^+CD25^+FoxP3^+H2Dd^+$), which were stained with anti-mouse CD4-APC, CD25-PE, FoxP3-PerCP, and H-2Dd-BV421. (B) Effects of IL-10 modRNA-based protein replacement on development of donor Treg chimerism. Immune cells were harvested from lymphoid organs and facial OMC allografts from both groups without immunosuppressive drugs on PODs 10–14. Donor immune cells were distinguished by staining anti-mouse H-2Dd-BV421 from recipient cells, which is specific for BALB/c cells. Subsequently, the amount of $H\text{-}2Dd^+$ donor Treg cells in blood, spleen, LNs, and facial OMC allografts was examined using flow cytometry. (C) Impact of IL-10 modRNA-based protein replacement on track of donor Tregs. Donor mandible from facial OMC allografts and recipient femurs were isolated in both groups without regimens on PODs 10–14 and analyzed using flow cytometry. Data were collected from four mice in both groups. Statistical data are represented as mean ± SD. IL-10 modRNA group (single 10 μg dose of IL-10 modRNA on POD 3) was compared with the buffer group for lymphoid organs and facial OMC allografts (*$p < 0.05$, Student's t test).

buffer group, suggesting that IL-10 modRNA induces donor Treg chimerism to protect allografts from alloimmunity-mediated rejection.

The modRNA technique is an efficient, safe, nonviral, integration-free, non-immunogenic, and footprint-free method for therapeutic protein replacement. It can facilitate immediate and rapid induction of *in vivo* target protein expression over a short period. Therefore, it has also been used in the development of vaccines against severe acute respiratory syndrome coronavirus-2 (SARS-CoV-2), such as the BNT and Moderna vaccines.[57] The technique has greatly shortened the time for the development of SARS-CoV-2 vaccines. Although conventional recombinant protein therapy has many advantages, such as fast delivery, immediate functioning, and controlled protein administration, recombinant protein has a very short half-life, in the range of 6 h *in vivo*, thus requiring repeat administration, and it cannot be delivered intracellularly. In addition, the cost of purifying recombinant protein is high, and the protocol is more difficult than for modRNA. Compared with conventional recombinant protein therapy, *in vivo* administration of therapeutic protein for various disease treatments is more easily achieved with modRNA. Therefore, modRNA-based therapeutic protein replacement holds great promise for the future of transplant medicine as well as in the treatment of other diseases.

Regarding the delivery system for modRNA, many materials can be used for encapsulating modRNA, such as lipid nanoparticles (LNPs), polymeric nanoparticles, and transfection reagents. In the development of modRNA-based vaccines, LNPs are the most commonly used system for delivery. Many studies have reported that LNPs possess the adjuvant ability to synergistically enhance pro-inflammatory, innate immunity, and anti-viral immune responses with the injection of LNP-formulated mRNA.[57,70–72] However, in transplant medicine, alloimmune responses must be suppressed in order to achieve immune balance between the recipient host and the donor allograft. Because of their detergent properties, widely used cationic lipid transfection reagents usually cause cell toxicity and necrosis through the disruption of membrane integrity.[59,73,74] Therefore, LNPs, with adjuvant properties, or cationic lipids, with detergent properties, were not a clear first choice for us in the delivery of modRNA in transplanted mice. The first studies using naked mRNA injections into skeletal muscle or hypothalamus without other transfection reagents resulted in direct target protein expression[75] or reversal of diabetes insipidus,[76] respectively. Use of saline or sucrose-citrate buffer formulated with luciferase modRNA was reported to have higher protein expression compared with the use of other transfection reagents such as RNAiMAX, Invivo-JetPEI, Invivofectamine, and calcium phosphate when modRNA complex was directly injected into mouse myocardium.[50] In addition, direct intracardiac injection of a citrate-saline buffer with

VEGF modRNA resulted in improved cardiac function.[48] Therefore, we tested saline buffer for encapsulating purified IL-10 modRNA and transient protein expression in face allotransplanted mice.

The survival rate of facial allografts in Figure 3 shows that two 5 μg doses of modRNA led to a longer subsequent period of survival than one 10 μg dose of modRNA. This may be due to IL-10 modRNA-induced transient protein expression. The pharmacokinetics of IL-10 modRNA-translated protein in mice by ELISA (Figure 2) showed that direct injection of 10 μg modRNA induced locally transient production for up to 10 days and a peak level at 24 h. Although a single 10 μg dose of IL-10 modRNA exhibited allograft protection against alloimmune responses, we found that a small part of tissue necrosis such as ears or tails in one mouse was observed and other five IL-10 modRNA-treated facial OMC allotransplanted mice did not appear tissue necrosis. Therefore, we used two 5 μg doses of IL-10 modRNA to observe the efficacy of facial allograft protection. Interestingly, repeat administration of the half dose significantly prolonged facial allograft survival compared with a single 10 μg dose. Moreover, the half dose of IL-10 modRNA completely did not cause tissue necrosis. In the pharmacokinetics of IL-10 modRNA-translated protein *in vivo* as shown in Figure 2, although two 5 μg doses of IL-10 modRNA produced around half concentrations of IL-10 protein compared with a single 10 μg dose of modRNA, it can induce locally transient expression for up to 20 days and produce two peak levels on days 1 and 13. Therefore, the sustained optimal concentration of IL-10 protein encoded by the IL-10 modRNA provides better protection against alloimmunity-mediated allograft destruction.

In our previous study, we demonstrated that the facial mandible of an allograft can induce donor chimerism in mice[61] as effectively as in rats.[69] Therefore, if a facial allograft contains a mandible, improved survival may be expected as a result of the induction of mixed chimerism compared with a facial allograft without a mandible. In this study, no matter which group (buffer, a single 10 μg dose of IL-10 modRNA, or two 5 μg doses of IL-10 modRNA), the survival rate of facial allografts with mandibles is dramatically enhanced compared with facial allografts without mandibles (Figure 3C). This suggests that donor bone marrow cells also contribute to prolonged survival of facial allografts. Moreover, we observed that donor chimerism was significantly enhanced in IL-10 modRNA-treated mice, and multilineage chimerism was even observed, such as in the appearance of T cells, B cells, DCs, NK cells, and macrophages in the blood, LNs, and facial OMC allografts (Figure 7). We speculate that IL-10 modRNA-translated protein creates an anti-inflammatory environment in face transplanted mice by suppressing pro-inflammatory Th1 cells in favor of expanded anti-inflammatory Treg cells in blood, LNs, and facial OMC allografts (Figure 6C). The anti-inflammatory environment in the host may provide an opportunity for induction and maintenance of donor immune cells and further achieve immune balance between host and donor. Subsequently, mixed chimerism developed in face transplanted mice, leading to facial allograft survival. Many studies have reported that anti-inflammatory strategies, such as anti-CD154/CTLA4Ig co-stimulation blockade, can prolong allograft survival by inducing mixed chimerism in animals or humans.[77–79] Moreover, hematologic multilineage chimerism was verified to induce organ allograft tolerance,[79,80] which is similar to our results showing a correlation between multilineage chimerism and facial allograft survival. More interestingly, we found that donor hematopoietic stem cells further differentiated to Treg cells and were harbored in the blood, LNs, donor mandible, and facial OMC allografts. Such local enrichment of allograft-residing donor Tregs may protect the allograft from host alloimmunity-mediated rejection. Similar evidence in organ transplantation has shown that Treg cells play a critical role in renal allograft tolerance via mixed chimerism.[80,81]

A study indicated that 5% of donor Tregs ($CD4^+CD25^+FoxP3^+$) appeared in recipient blood within the first week after liver allotransplantation,[82] which is similar to our results that 10.7% of donor Tregs in the blood of IL-10 modRNA-treated mice compared with 0.35% of buffer group (Figure 8B). Moreover, isolated donor Tregs from liver allotransplanted patients suppressed lymphocyte proliferation and IFN-γ production of donor and recipient T cells. They demonstrated that donor Tregs directly inhibit the alloimmune responses and help mixed chimerism-induced allograft tolerance early after liver allotransplantation. Another study demonstrated that posttransplantation cyclophosphamide-induced GVHD protection requires donor $CD4^+CD25^+FoxP3^+$ Tregs to suppress alloimmune responses in addition to the depletion of alloreactive T cells.[83]

Therefore, this study inspires the idea that the local administration of IL-10 modRNA monotherapy may also provide good protection in other organ allotransplantations. If IL-10 modRNA monotherapy is combined with bone marrow transplantation, it may increase the efficacy of prolonged survival compared with IL-10 monotherapy. However, the doses of IL-10 modRNA need to be evaluated in different animal models. A study showed that low doses of IL-10 had good protection for GVHD, while high doses accelerated GVHD lethality.[42] This result is similar to our result that low doses of IL-10 modRNA displayed better protection against allograft destruction than the high dose. If IL-10 modRNA therapy is combined with a short-term systemic immunosuppressive regimen in transplantation, the doses of immunosuppressive drugs may be reduced. Moreover, the local administration of IL-10 modRNA may decrease the side effects of systemic administration in addition to the reduction of immunosuppressive drugs. This study thus provides valuable information regarding the efficacy of IL-10 modRNA monotherapy on composite vascularized allotransplantation, allowing us to further understand the potential application of IL-10 modRNA-based protein replacement therapy in other pro-inflammatory diseases.

MATERIALS AND METHODS

IL-10 modRNA synthesis

Mouse IL-10 (FLAG tag) plasmid (GeneBank: NM_010548) was purchased from OriGene Technologies. IL-10 cDNA with FLAG or not was first cloned into the RNA synthesis vector using a Gibson Assembly cloning kit (New England Biolabs, Ipswich, MA), including

a 5′ exonuclease to generate long overhangs, a polymerase to fill gaps in annealed single-stranded regions, and a DNA ligase to seal gaps in annealed and filled gaps. The robust T7 RNA polymerase was used for *in vitro* transcription of IL-10 modRNA from a linearized DNA template (RNA synthesis vector) that included sequences for mouse IL-10 cDNA, 5′ UTR Kozak consensus, 3′ UTRs, and poly-A tail. Anti-reverse cap analogs and modified nucleotides, such as pseudouridine (Ψ)-5′-triphosphate and 5-methylcytidine-5′-triphosphate, were incorporated into the modRNAs to decrease the immune response of host cells and increase mRNA stability. Following modRNA synthesis, the DNA template was digested using DNase I. In addition, the 5′ triphosphates of modRNA ends were removed by phosphatase for decreased innate immunity in the host. Purified modRNA was formulated in saline buffer according to the designated concentration after RNA purification.

In vitro protein assay for IL-10 modRNA

Protein translation from modRNA was confirmed in different cell types, including mouse embryonic fibroblasts, C2C12 mouse muscle myoblasts, human embryonic kidney 293 (HEK293) cells, and Jurkat cells (clone E6-1, human T cells), which were used to transfect IL-10 modRNA. These cells were purchased from Bioresources Collection and Research Center (BCRC). MEF (2×10^4 cells per well), C2C12 (1×10^5 cells per well), and 293 (1×10^5 cells per well) cells were transfected with 100 ng purified modRNA (GFP or IL-10). Jurkat cells (5×10^5 cells per well) were transfected with 200 ng purified modRNA (GFP or IL-10). GFP modRNA (catalog no. MR700A-1) was purchased from SBI System Biosciences. These cells were transfected with purified IL-10 modRNA in 96-well flat plates using Lipofectamine 3000 (Thermo Fisher Scientific, Carlsbad, CA). At 6, 24, and 48 h, the supernatants were harvested, and concentrations of secreted IL-10 were determined using a mouse IL-10 ELISA kit (R&D Systems, Minneapolis, MN). A SpectraMax reader was used to read the absorbance at 450 nm.

Western blot

Twenty micrograms of protein was analyzed by loading on 12% SDS-PAGE, and electrophoresis was carried out using SDS running buffer (Thermo Fisher Scientific). Fractionated protein was electroblotted onto a polyvinylidene difluoride membrane. Then, 5% BSA in 0.1% Tween-TBS buffer was used to block the membrane, and mouse IL-10 primary antibody (dilution 1:1,000; GeneTex, Irvine, CA) was added followed by incubation for 2 h. Subsequently, horseradish peroxidase (HRP)-labeled secondary antibody (dilution 1:5,000; GeneTex) was added to the membrane followed by incubation for 1 h, and ECL western blotting substrate (Thermo Fisher Scientific) was added for immunoreaction. The ChemiDoc Touch Imaging System (Bio-Rad, Hercules, CA) was used to visualize chemiluminescent signals.

In vitro functional assay for IL-10 modRNA

The *in vitro* functional ability of IL-10 modRNA-translated proteins was examined in a T cell line (Jurkat, clone E6-1, BCRC-60424). Jurkat cells (3×10^5 cells per well) were transfected with 200 ng IL-10 modRNA and seeded in the top chambers of Corning HTS Transwell 96-well plates (Merck, Darmstadt, Germany). Mouse C57BL/6J splenocytes (3×10^5 cells per well) were activated with coated anti-mouse CD3 (2 μg/mL; BioLegend, San Diego, CA) and soluble anti-mouse CD28 (2 μg/mL; BioLegend) and seeded in the bottom reservoir. At different time points, the supernatants in the bottom reservoir were harvested and analyzed by mouse IL-2 and IFN-γ ELISA (R&D Systems) according to the manufacturer's instructions. A SpectraMax reader was used to read the absorbance at 450 nm.

Quantification of exogenous IL-10 protein in tissues

To evaluate exogenous protein expression of IL-10 *in vivo* after direct injection in tissue, purified IL-10_FLAG modRNA was used. Additionally, in order to examine expression time of exogenous IL-10 protein, two dose groups of IL-10_FLAG modRNA were designed in the experiments. modRNA diluted in 50 μL saline buffer was directly injected in the right semi-face tissue after male C57BL/6J mice (10–12 weeks old) were anesthetized with 1.5%–2% isoflurane. A single 10 μg dose of purified IL-10_FLAG modRNA formulated in 50 μL saline buffer was directly injected into right face tissue at day 0, defined as the IL-10 modRNA-10 group. Two 5 μg doses of purified IL-10_FLAG modRNA formulated in 50 μL saline buffer was directly injected into right face tissue at day 0 and day 12, defined as the IL-10 modRNA-5 group. At the designated time points after modRNA injection, various tissues were harvested, including blood serum, spleen, LNs near the injected tissue, and injected tissue. Spleen, LN, or 100 μg face tissue was added to 400 μL T-PER Tissue Protein Extraction Reagent (Thermo Fisher Scientific). We added ceramic beads (3 mm) to the tissues for homogenization using a Precellys homogenizer. The homogenate was centrifuged at 14,000 × *g* for 15 min, and the supernatants were analyzed by ELISA. The concentration of exogenous IL-10_FLAG fusion protein in various tissues was measured using FLAG ELISA kit (Cayman Chemical, Ann Arbor, MI) according to the manufacturer's instructions. A SpectraMax reader was used to read the absorbance at 450 nm.

Immunohistochemistry of exogenous IL-10 protein

One 50 μL dose of saline buffer or 10 μg IL-10_FLAG modRNA diluted in 50 μL saline buffer was directly injected in the right semi-face tissue after male C57BL/6J mice (10–12 weeks old) were anesthetized with 1.5%–2% isoflurane. After 2 days, the injected face tissue was harvested and put in 4% formaldehyde for fixation. The injected tissue was transversely sectioned and distally incised 2 mm in both directions. The sections were embedded in paraffin and cut into 4 μm slices. Antigen retrieval was performed in Ventana Cell Conditioner 1 at 95°C. The BOND Polymer Refine detection system (Leica Biosystems, Buffalo Grove, IL) was used for immunohistochemistry. Primary antibodies were used against FLAG (dilution 1:200; Sigma-Aldrich, Louis, MO) with incubation for 2 h at 37°C. Post-primary rabbit anti-mouse (<10 μg/mL) was added, followed by polymer anti-rabbit HRP (<25 μg/mL). Expression of IL-10_FLAG fusion protein in injected tissue was indicated by DAB chromogenic brown reagent.

Immunohistochemistry of CD3 and FoxP3

Immunohistochemical studies were performed on formalin-fixed, paraffin-embedded tissue. Tissue sections were deparaffinized according to established procedures. Antigen retrieval was performed at pH9.0 using Epitope Retrieval 2 solution (Leica Microsystems, Wetzlar, Germany) for 40 min at 100°C. Primary antibodies were used against CD3 (SP7 clone; dilution 1:100; GeneTex) or FoxP3 (FJK-16 s clone; dilution 1:200; Thermo Fisher Scientific for 60 min. Slides were then stained using the Leica Microsystems BONDMAX autostainer according to the following steps. Secondary antibodies (goat anti-rabbit poly-AP IgG reagent localized rabbit antibody) were used against CD3 antibodies for 40 min. Additionally, secondary antibodies (rabbit anti-rat poly-AP IgG reagent localized rat antibody) were used against FoxP3 antibodies for 40 min. Staining was developed with the substrate chromogen, fast red for 10 min. The sections were counterstained with modified Mayer's hematoxylin for 5 min.

Mice

C57BL/6J and BALB/c mice (6–8 weeks old) were purchased from the National Laboratory Animal Center, Taiwan, and used as recipients and donors, respectively. Ketoprofen (2.5 mg/kg/day), a pain medicine, and cefazolin (50 mg/day), an antibiotic, were subcutaneously injected into postoperative mice for 3 days. These mice were cared for in a comfortable environment with abundant nesting materials. All mouse protocols followed in the study were in full compliance with the recommendations set forth in the Guide for the Care and Use of Laboratory Animals of the Chang Gung Memorial Hospital. Mouse protocols were approved by the Committee on the Ethics of Animal Experiments of the Chang Gung Memorial Hospital and its Institutional Animal Care and Use Committee (IACUC) under permit numbers IACUC 2019120201, IACUC 2020121608, IACUC 20210315032, and IACUC 2021091405.

Heterotopic face transplantation

We established a microsurgical protocol for heterotopic face transplantation in a mouse model.[60] The right side of the donor face was harvested and implanted into the right neck of recipient mice. For anesthesia, ketamine and rocuronium were intraperitoneally injected in the donor mice because of the need for sacrifice, and isoflurane into the recipient mice to maintain survival. The composite vascularized facial flap contained upper lips, lower lips, right commissure, cheek (skin and mucosa), right hemi-mandible with two central incisors, masseter muscle, anterior facial vein, and carotid artery. In the donor surgery, carotid artery and anterior facial vein were carefully ligated after the dissection and ligation of all graft branches. As the blood vessels of mice range 0.2–0.4 mm in diameter, the hands-on suture technique seemed was considered unsuitable for vascular anastomosis. Therefore, a polyamide cuff was used for vascular anastomosis in the mice in this study. The semi-face graft was cut and included upper and lower lips, with mandibular osteotomy of incisor teeth, mouth muscle, and mucosa. In the recipient surgery, the submandibular gland in the right neck was removed, and the anterior facial vein was ligated. After fixation of the face graft on the neck space, artery anastomosis was performed between the donor and recipient common carotid arteries; vein anastomosis was performed between the anterior and posterior facial veins using the cuff technique.[84,85] The success of face grafting was confirmed on the basis of whether blood perfusion was adequate, and the skin was then sutured using 6-0 nylon suture.

Postoperative care

Postoperative mice were subcutaneously injected with cephazolin (50 mg/kg/day), ketoprofen (1 mg/kg/day), and saline (30 mL/kg/day) for 3 days. Buffer saline or IL-10 modRNA (10 or 5 μg) diluted in saline was subcutaneously injected around the facial allografts in 3 separate sites (50 μL each, total volume 150 μL). Imaging, weight measurement, and visual inspection of each mouse were performed daily to collect data on facial allograft survival. Rejection time was defined by the appearance of epidermolysis or diffuse erythema to complete necrosis of the allograft.

Histological evaluation

H&E staining was used to evaluate the degree of lymphocyte infiltration into facial OMC allografts as a result of the host's alloimmune responses. Facial OMC allografts containing skin and muscle in buffer and IL-10 modRNA groups were collected on PODs 10–14 and stained with histological H&E.

Quantitation of cytokine proteins by Luminex multiplex assays

Spleen, LNs near OMC allografts, and facial OMC allografts were harvested on PODs 10–14 in buffer and IL-10 modRNA-treated face allotransplanted mice (single 10 μg dose of IL-10 modRNA on POD 3) without any immunosuppressive drugs. 100 mg of tissue samples were incubated with RIPA buffer and then shredded for ultrasonication. Shredded tissues were centrifugated at 16,000 × *g* for 10 min. Collected supernatants were analyzed for various cytokine measurements such as IL-12, IFN-γ, TNF-α, IL-1β, IL-2, IL-17, IL-4, and IL-10 using a ProcartaPlex multiplex assay kit on a Luminex instrument platform (Thermo Fisher Scientific). The ProcartaPlex multiplex assay analyzes cytokine measurements similar to the conventional ELISA assay but with greater efficiency and a little sample.

Purification of facial allograft-infiltrated cells

Facial OMC allografts with mandible removed were collected and finely cut into small pieces using dissection scissors. Digestion buffer (3 mL) containing collagenase type IV (0.8 mg/mL; Worthington, Lakewood, NJ), 10% FBS, 1% HEPES, 1% penicillin/streptavidin, and DNAse (0.02 mg/mL; Sigma-Aldrich) in PBS was added to shredded tissues. Mixtures were incubated at 37°C for 1 h and washed with buffer (2% FBS and 1% penicillin in PBS), then filtered using a 100 μm filter and centrifuged at 1,200 rpm for 5 min. Ficoll gradient centrifugation was performed for cell isolation and flow cytometry was used to analyze the cell composition.

Flow cytometry

Isolated immune cells were analyzed by staining fluorescence conjugated antibodies against cell surface markers and intracellular proteins. Anti-mouse CD4-APC, anti-mouse CD19-APC, anti-mouse

H-2Dd-BV421, anti-mouse H-2Db-FITC, anti-mouse CD8a-PE, anti-mouse NK-1.1-PE-Cy7, and anti-mouse IFN-γ-PerCP-Cy5.5 antibodies were purchased from BD Biosciences (San Jose, CA). Anti-mouse CD11c-APC, anti-mouse FoxP3-PerCP, and anti-mouse CD25-PE antibodies were purchased from eBioscience (San Diego, CA). Anti-mouse CD11b-PE antibody was purchased from Miltenyi Biotec (Bergisch Gladbach, Germany). For Treg cell staining, immune cells were first stained with cell surface markers CD4 and CD25 and fixed overnight at 4°C, then permeabilized for 30 min at room temperature, and finally stained with intracellular FoxP3 for 30 min. For T helper cell intracellular cytokine staining (Th1, Th17, and Th2 cells), immune cells were first activated in the presence of phorbol 12-myristate 13-acetate (20 ng/mL), ionomycin (1 μg/mL), and monesine (4 μM) for 4 h, and then staining of cell surface and intracellular cytokines was carried out.

Statistical analysis

All data in this study are expressed as mean ± SD. The Kaplan-Meier method was used to calculate the statistical significance of facial survival rate by comparing the differences using the log rank test. The two-tailed Student's t test was used to measure significant differences between various groups. GraphPad Prism 6 software was used to perform all calculations. p values <0.05 were considered to indicate statistical significance.

DATA AVAILABILITY

The authors confirm that the data supporting the findings of this study are available within the article and its supplemental information. Additionally, the data that support the findings of this study are available from the corresponding author (A.Y.L.W., aline2355@yahoo.com.tw), upon reasonable request.

SUPPLEMENTAL INFORMATION

Supplemental information can be found online at https://doi.org/10.1016/j.omtn.2023.02.016.

ACKNOWLEDGMENTS

We thank the Laboratory Animal Center at Chang Gung Memorial Hospital, Taiwan (received AAALAC full accreditation), for animal care and IVIS. We also thank the Center for Artificial Intelligence in Medicine, Chang Gung Memorial Hospital, Taiwan, for histological slide scanning using NanoZoomer S360 Digital slide scanner, which was supported by grant CLRPG3H0015. Additionally, this study was supported by grants from the Chang Gung Medical Foundation, Chang Gung Memorial Hospital, Taiwan (CMRPG1H0083, CMRPG1L0041, CMRPG3M0281, and CMRPG3M0282), and the Ministry of Science and Technology, Taiwan (MOST 108-2314-B-182A-009, MOST 109-2314-B-182A-056-MY3, and MOST 110-2314-B-182A-137-MY3). All authors have reviewed and approved the final manuscript.

AUTHOR CONTRIBUTIONS

Conceptualization, A.Y.L.W.; Methodology, A.E.A., D.D.P., K.-H.C., C.-M.L., and C.-H.L.; Investigation, A.E.A., D.D.P., K.-H.C., C.-M.L., and C.-H.L.; Writing – Original Draft, A.E.A. and A.Y.L.W.; Writing – Review & Editing, A.Y.L.W., S.-C.H., Y.-C.C., and F.-C.W.; Supervision, A.Y.L.W. and F.-C.W.; Funding Acquisition, A.Y.L.W. and F.-C.W.

DECLARATION OF INTERESTS

The authors declare no competing interests.

REFERENCES

1. Kaufman, C.L., Ouseph, R., Blair, B., Kutz, J.E., Tsai, T.M., Scheker, L.R., Tien, H.Y., Moreno, R., Ozyurekoglu, T., Banegas, R., et al. (2012). Graft vasculopathy in clinical hand transplantation. Am. J. Transplant. *12*, 1004–1016. https://doi.org/10.1111/j.1600-6143.2011.03915.x.

2. Hautz, T., Zelger, B., Grahammer, J., Krapf, C., Amberger, A., Brandacher, G., Landin, L., Müller, H., Schön, M.P., Cavadas, P., et al. (2010). Molecular markers and targeted therapy of skin rejection in composite tissue allotransplantation. Am. J. Transplant. *10*, 1200–1209. https://doi.org/10.1111/j.1600-6143.2010.03075.x.

3. Landin, L., Bonastre, J., Casado-Sanchez, C., Diez, J., Ninkovic, M., Lanzetta, M., del Bene, M., Schneeberger, S., Hautz, T., Lovic, A., et al. (2012). Outcomes with respect to disabilities of the upper limb after hand allograft transplantation: a systematic review. Transpl. Int. *25*, 424–432. https://doi.org/10.1111/j.1432-2277.2012.01433.x.

4. Carlsen, B.T., Prigge, P., and Peterson, J. (2014). Upper extremity limb loss: functional restoration from prosthesis and targeted reinnervation to transplantation. J. Hand Ther. *27*, 106–113. https://doi.org/10.1016/j.jht.2013.10.007.

5. Lee, W.P.A. (2017). Hand transplantation: evolution of a personal outlook. J. Hand Surg. Am. *42*, 286–290. https://doi.org/10.1016/j.jhsa.2017.01.019.

6. Park, S.H., Eun, S.C., and Kwon, S.T. (2019). Hand transplantation: current status and immunologic obstacles. Exp. Clin. Transplant. *17*, 97–104. https://doi.org/10.6002/ect.2018.0163.

7. Shores, J.T., Malek, V., Lee, W.P.A., and Brandacher, G. (2017). Outcomes after hand and upper extremity transplantation. J. Mater. Sci. Mater. Med. *28*, 72. https://doi.org/10.1007/s10856-017-5880-0.

8. Wilks, D.J., Clark, B., and Kay, S.P.J. (2020). The histocompatibility and immunogenetics of hand transplantation. Int. J. Immunogenet. *47*, 24–27. https://doi.org/10.1111/iji.12469.

9. Sosin, M., and Rodriguez, E.D. (2016). The face transplantation update: 2016. Plast. Reconstr. Surg. *137*, 1841–1850. https://doi.org/10.1097/PRS.0000000000002149.

10. Smeets, R., Rendenbach, C., Birkelbach, M., Al-Dam, A., Gröbe, A., Hanken, H., and Heiland, M. (2014). Face transplantation: on the verge of becoming clinical routine? BioMed Res. Int. *2014*, 907272. https://doi.org/10.1155/2014/907272.

11. Kueckelhaus, M., Lehnhardt, M., Fischer, S., Eriksson, E., Pomahac, B., and Hirsch, T. (2014). [Progress in face transplantation]. Handchir. Mikrochir. Plast. Chir. *46*, 206–213. https://doi.org/10.1055/s-0034-1385850.

12. Siemionow, M., Gharb, B.B., and Rampazzo, A. (2011). Pathways of sensory recovery after face transplantation. Plast. Reconstr. Surg. *127*, 1875–1889. https://doi.org/10.1097/PRS.0b013e31820e90c3.

13. Kollar, B., and Pomahac, B. (2018). Facial restoration by transplantation. Surgeon *16*, 245–249. https://doi.org/10.1016/j.surge.2018.01.003.

14. Aycart, M.A., Kiwanuka, H., Krezdorn, N., Alhefzi, M., Bueno, E.M., Pomahac, B., and Oser, M.L. (2017). Quality of life after face transplantation: outcomes, assessment tools, and future directions. Plast. Reconstr. Surg. *139*, 194–203. https://doi.org/10.1097/PRS.0000000000002890.

15. Siemionow, M., Gharb, B.B., and Rampazzo, A. (2013). Successes and lessons learned after more than a decade of upper extremity and face transplantation. Curr. Opin. Organ Transplant. *18*, 633–639. https://doi.org/10.1097/MOT.0000000000000021.

16. Breidenbach, W.C., Meister, E.A., Becker, G.W., Turker, T., Gorantla, V.S., Hassan, K., and Kaplan, B. (2016). A statistical comparative assessment of face and hand transplantation outcomes to determine whether either meets the standard of care threshold. Plast. Reconstr. Surg. *137*, 214e–222e. https://doi.org/10.1097/PRS.0000000000001893.

17. Siemionow, M. (2016). The miracle of face transplantation after 10 years. Br. Med. Bull. *120*, 5–14. https://doi.org/10.1093/bmb/ldw045.

18. Wang, A.Y.L., and Loh, C.Y.Y. (2018). Reviewing immunosuppressive regimens in animal models for vascularized composite allotransplantation. Plast. Aesthet. Res. *5*, 10. https://doi.org/10.20517/2347-9264.2017.90.

19. Lao, W.W., Wang, Y.L., Ramirez, A.E., Cheng, H.Y., and Wei, F.C. (2014). A new rat model for orthotopic abdominal wall allotransplantation. Plast. Reconstr. Surg. Glob. Open *2*, e136. https://doi.org/10.1097/GOX.0000000000000086.

20. Fryer, M., Grahammer, J., Khalifian, S., Furtmüller, G.J., Lee, W.P.A., Raimondi, G., and Brandacher, G. (2015). Exploring cell-based tolerance strategies for hand and face transplantation. Expert Rev. Clin. Immunol. *11*, 1189–1204. https://doi.org/10.1586/1744666X.2015.1078729.

21. Leonard, D.A., Gordon, C.R., Sachs, D.H., and Cetrulo, C.L., Jr. (2012). Immunobiology of face transplantation. J. Craniofac. Surg. *23*, 268–271. https://doi.org/10.1097/SCS.0b013e318241b8e0.

22. Anggelia, M.R., Cheng, H.Y., Lai, P.C., Hsieh, Y.H., Lin, C.H., and Lin, C.H. (2022). Cell therapy in vascularized composite allotransplantation. Biomed. J. *45*, 454–464. https://doi.org/10.1016/j.bj.2022.01.005.

23. Lee, W.P., Yaremchuk, M.J., Pan, Y.C., Randolph, M.A., Tan, C.M., and Weiland, A.J. (1991). Relative antigenicity of components of a vascularized limb allograft. Plast. Reconstr. Surg. *87*, 401–411. https://doi.org/10.1097/00006534-199103000-00001.

24. Hattori, T., Saban, D.R., Emami-Naeini, P., Chauhan, S.K., Funaki, T., Ueno, H., and Dana, R. (2012). Donor-derived, tolerogenic dendritic cells suppress immune rejection in the indirect allosensitization-dominant setting of corneal transplantation. J. Leukoc. Biol. *91*, 621–627. https://doi.org/10.1189/jlb.1011500.

25. Ezzelarab, M., and Thomson, A.W. (2011). Tolerogenic dendritic cells and their role in transplantation. Semin. Immunol. *23*, 252–263. https://doi.org/10.1016/j.smim.2011.06.007.

26. Natarajan, S., and Thomson, A.W. (2010). Tolerogenic dendritic cells and myeloid-derived suppressor cells: potential for regulation and therapy of liver auto- and alloimmunity. Immunobiology *215*, 698–703. https://doi.org/10.1016/j.imbio.2010.05.024.

27. Morelli, A.E., and Thomson, A.W. (2007). Tolerogenic dendritic cells and the quest for transplant tolerance. Nat. Rev. Immunol. *7*, 610–621. https://doi.org/10.1038/nri2132.

28. Ireland, S.J., Monson, N.L., and Davis, L.S. (2015). Seeking balance: potentiation and inhibition of multiple sclerosis autoimmune responses by IL-6 and IL-10. Cytokine *73*, 236–244. https://doi.org/10.1016/j.cyto.2015.01.009.

29. Moore, K.W., de Waal Malefyt, R., Coffman, R.L., and O'Garra, A. (2001). Interleukin-10 and the interleukin-10 receptor. Annu. Rev. Immunol. *19*, 683–765. https://doi.org/10.1146/annurev.immunol.19.1.683.

30. Varma, T.K., Toliver-Kinsky, T.E., Lin, C.Y., Koutrouvelis, A.P., Nichols, J.E., and Sherwood, E.R. (2001). Cellular mechanisms that cause suppressed gamma interferon secretion in endotoxin-tolerant mice. Infect. Immun. *69*, 5249–5263. https://doi.org/10.1128/IAI.69.9.5249-5263.2001.

31. Bondeson, J., Browne, K.A., Brennan, F.M., Foxwell, B.M., and Feldmann, M. (1999). Selective regulation of cytokine induction by adenoviral gene transfer of IkappaBalpha into human macrophages: lipopolysaccharide-induced, but not zymosan-induced, proinflammatory cytokines are inhibited, but IL-10 is nuclear factor-kappaB independent. J. Immunol. *162*, 2939–2945. https://doi.org/10.4049/jimmunol.162.5.2939.

32. Opp, M.R., Smith, E.M., and Hughes, T.K., Jr. (1995). Interleukin-10 (cytokine synthesis inhibitory factor) acts in the central nervous system of rats to reduce sleep. J. Neuroimmunol. *60*, 165–168. https://doi.org/10.1016/0165-5728(95)00066-b.

33. Aste-Amezaga, M., Ma, X., Sartori, A., and Trinchieri, G. (1998). Molecular mechanisms of the induction of IL-12 and its inhibition by IL-10. J. Immunol. *160*, 5936–5944. https://doi.org/10.4049/jimmunol.160.12.5936.

34. Chen, W., Jin, W., Hardegen, N., Lei, K.J., Li, L., Marinos, N., McGrady, G., and Wahl, S.M. (2003). Conversion of peripheral CD4+CD25- naive T cells to CD4+CD25+ regulatory T cells by TGF-beta induction of transcription factor Foxp3. J. Exp. Med. *198*, 1875–1886. https://doi.org/10.1084/jem.20030152.

35. Zhang, G.Y., Hu, M., Wang, Y.M., and Alexander, S.I. (2009). Foxp3 as a marker of tolerance induction versus rejection. Curr. Opin. Organ Transplant. *14*, 40–45. https://doi.org/10.1097/MOT.0b013e32831da83c.

36. Ziegler, S.F. (2006). FOXP3: of mice and men. Annu. Rev. Immunol. *24*, 209–226. https://doi.org/10.1146/annurev.immunol.24.021605.090547.

37. Tahvildari, M., Emami-Naeini, P., Omoto, M., Mashaghi, A., Chauhan, S.K., and Dana, R. (2017). Treatment of donor corneal tissue with immunomodulatory cytokines: a novel strategy to promote graft survival in high-risk corneal transplantation. Sci. Rep. *7*, 971. https://doi.org/10.1038/s41598-017-01065-z.

38. Zhang, Y.C., Pileggi, A., Agarwal, A., Molano, R.D., Powers, M., Brusko, T., Wasserfall, C., Goudy, K., Zahr, E., Poggioli, R., et al. (2003). Adeno-associated virus-mediated IL-10 gene therapy inhibits diabetes recurrence in syngeneic islet cell transplantation of NOD mice. Diabetes *52*, 708–716. https://doi.org/10.2337/diabetes.52.3.708.

39. Goudy, K., Song, S., Wasserfall, C., Zhang, Y.C., Kapturczak, M., Muir, A., Powers, M., Scott-Jorgensen, M., Campbell-Thompson, M., Crawford, J.M., et al. (2001). Adeno-associated virus vector-mediated IL-10 gene delivery prevents type 1 diabetes in NOD mice. Proc. Natl. Acad. Sci. USA *98*, 13913–13918. https://doi.org/10.1073/pnas.251532298.

40. Nitta, Y., Tashiro, F., Tokui, M., Shimada, A., Takei, I., Tabayashi, K., and Miyazaki, J. (1998). Systemic delivery of interleukin 10 by intramuscular injection of expression plasmid DNA prevents autoimmune diabetes in nonobese diabetic mice. Hum. Gene Ther. *9*, 1701–1707. https://doi.org/10.1089/hum.1998.9.12-1701.

41. Abraham, S., Choi, J.G., Ye, C., Manjunath, N., and Shankar, P. (2015). IL-10 exacerbates xenogeneic GVHD by inducing massive human T cell expansion. Clin. Immunol. *156*, 58–64. https://doi.org/10.1016/j.clim.2014.11.004.

42. Blazar, B.R., Taylor, P.A., Panoskaltsis-Mortari, A., Narula, S.K., Smith, S.R., Roncarolo, M.G., and Vallera, D.A. (1998). Interleukin-10 dose-dependent regulation of CD4+ and CD8+ T cell-mediated graft-versus-host disease. Transplantation *66*, 1220–1229. https://doi.org/10.1097/00007890-199811150-00018.

43. Blazar, B.R., Taylor, P.A., Smith, S., and Vallera, D.A. (1995). Interleukin-10 administration decreases survival in murine recipients of major histocompatibility complex disparate donor bone marrow grafts. Blood *85*, 842–851. https://doi.org/10.1182/blood.V85.3.842.bloodjournal853842.

44. Wang, A.Y.L. (2021). Application of modified mRNA in somatic reprogramming to pluripotency and directed conversion of cell fate. Int. J. Mol. Sci. *22*, 8148. https://doi.org/10.3390/ijms22158148.

45. Stepinski, J., Waddell, C., Stolarski, R., Darzynkiewicz, E., and Rhoads, R.E. (2001). Synthesis and properties of mRNAs containing the novel "anti-reverse" cap analogs 7-methyl(3'-O-methyl)GpppG and 7-methyl (3'-deoxy)GpppG. RNA *7*, 1486–1495.

46. Warren, L., Manos, P.D., Ahfeldt, T., Loh, Y.H., Li, H., Lau, F., Ebina, W., Mandal, P.K., Smith, Z.D., Meissner, A., et al. (2010). Highly efficient reprogramming to pluripotency and directed differentiation of human cells with synthetic modified mRNA. Cell Stem Cell *7*, 618–630. https://doi.org/10.1016/j.stem.2010.08.012.

47. Magadum, A., Kaur, K., and Zangi, L. (2019). mRNA-based protein replacement therapy for the heart. Mol. Ther. *27*, 785–793. https://doi.org/10.1016/j.ymthe.2018.11.018.

48. Carlsson, L., Clarke, J.C., Yen, C., Gregoire, F., Albery, T., Billger, M., Egnell, A.C., Gan, L.M., Jennbacken, K., Johansson, E., et al. (2018). Biocompatible, purified VEGF-A mRNA improves cardiac function after intracardiac injection 1 Week post-myocardial infarction in swine. Mol. Ther. Methods Clin. Dev. *9*, 330–346. https://doi.org/10.1016/j.omtm.2018.04.003.

49. Singh, R.D., Hillestad, M.L., Livia, C., Li, M., Alekseev, A.E., Witt, T.A., Stalboerger, P.G., Yamada, S., Terzic, A., and Behfar, A. (2019). M(3)RNA drives targeted gene delivery in acute myocardial infarction. Tissue Eng. Part A *25*, 145–158. https://doi.org/10.1089/ten.TEA.2017.0445.

50. Sultana, N., Magadum, A., Hadas, Y., Kondrat, J., Singh, N., Youssef, E., Calderon, D., Chepurko, E., Dubois, N., Hajjar, R.J., and Zangi, L. (2017). Optimizing cardiac delivery of modified mRNA. Mol. Ther. *25*, 1306–1315. https://doi.org/10.1016/j.ymthe.2017.03.016.

51. Creusot, R.J., Chang, P., Healey, D.G., Tcherepanova, I.Y., Nicolette, C.A., and Fathman, C.G. (2010). A short pulse of IL-4 delivered by DCs electroporated with

modified mRNA can both prevent and treat autoimmune diabetes in NOD mice. Mol. Ther. *18*, 2112–2120. https://doi.org/10.1038/mt.2010.146.

52. Sahu, I., Haque, A.K.M.A., Weidensee, B., Weinmann, P., and Kormann, M.S.D. (2019). Recent developments in mRNA-based protein supplementation therapy to target lung diseases. Mol. Ther. *27*, 803–823. https://doi.org/10.1016/j.ymthe.2019.02.019.

53. Walsh, E.E., Frenck, R.W., Jr., Falsey, A.R., Kitchin, N., Absalon, J., Gurtman, A., Lockhart, S., Neuzil, K., Mulligan, M.J., Bailey, R., et al. (2020). Safety and immunogenicity of two RNA-based covid-19 vaccine candidates. N. Engl. J. Med. *383*, 2439–2450. https://doi.org/10.1056/NEJMoa2027906.

54. Polack, F.P., Thomas, S.J., Kitchin, N., Absalon, J., Gurtman, A., Lockhart, S., Perez, J.L., Pérez Marc, G., Moreira, E.D., Zerbini, C., et al. (2020). Safety and efficacy of the BNT162b2 mRNA covid-19 vaccine. N. Engl. J. Med. *383*, 2603–2615. https://doi.org/10.1056/NEJMoa2034577.

55. Jackson, L.A., Anderson, E.J., Rouphael, N.G., Roberts, P.C., Makhene, M., Coler, R.N., McCullough, M.P., Chappell, J.D., Denison, M.R., Stevens, L.J., et al. (2020). An mRNA vaccine against SARS-CoV-2 - preliminary report. N. Engl. J. Med. *383*, 1920–1931. https://doi.org/10.1056/NEJMoa2022483.

56. Baden, L.R., El Sahly, H.M., Essink, B., Kotloff, K., Frey, S., Novak, R., Diemert, D., Spector, S.A., Rouphael, N., Creech, C.B., et al. (2021). Efficacy and safety of the mRNA-1273 SARS-CoV-2 vaccine. N. Engl. J. Med. *384*, 403–416. https://doi.org/10.1056/NEJMoa2035389.

57. Wang, A.Y.L. (2022). Modified mRNA-based vaccines against coronavirus disease 2019. Cell Transplant. *31*. 9636897221090259. https://doi.org/10.1177/09636897221090259.

58. Zangi, L., Lui, K.O., von Gise, A., Ma, Q., Ebina, W., Ptaszek, L.M., Später, D., Xu, H., Tabebordbar, M., Gorbatov, R., et al. (2013). Modified mRNA directs the fate of heart progenitor cells and induces vascular regeneration after myocardial infarction. Nat. Biotechnol. *31*, 898–907. https://doi.org/10.1038/nbt.2682.

59. Xue, H.Y., Liu, S., and Wong, H.L. (2014). Nanotoxicity: a key obstacle to clinical translation of siRNA-based nanomedicine. Nanomedicine (Lond) *9*, 295–312. https://doi.org/10.2217/nnm.13.204.

60. Cardona, E., Wang, A.Y.L., Loh, C.Y.Y., Chuang, S.H., Lee, C.M., ALDeek, N., Lin, C.H., and Wei, F.C. (2019). A new face subunit transplant model in mice, containing skin, mandible, and oral mucosa for future face vascularized composite allotransplantation studies. Plast. Reconstr. Surg. *144*, 115–123. https://doi.org/10.1097/PRS.0000000000005774.

61. De Paz, D., Aviña, A.E., Cardona, E., Lee, C.M., Lin, C.H., Lin, C.H., Wei, F.C., and Wang, A.Y.L. (2021). The mandible ameliorates facial allograft rejection and is associated with the development of regulatory T cells and mixed chimerism. Int. J. Mol. Sci. *22*, 11104. https://doi.org/10.3390/ijms222011104.

62. Issa, F., Schiopu, A., and Wood, K.J. (2010). Role of T cells in graft rejection and transplantation tolerance. Expert Rev. Clin. Immunol. *6*, 155–169. https://doi.org/10.1586/eci.09.64.

63. Siemionow, M., and Klimczak, A. (2008). Basics of immune responses in transplantation in preparation for application of composite tissue allografts in plastic and reconstructive surgery: part I. Plast. Reconstr. Surg. *121*, 4e–12e. https://doi.org/10.1097/01.prs.0000299470.95855.ce.

64. Wang, A.Y.L., Loh, C.Y.Y., Chen, S.J., Kao, H.K., Lin, C.H., Chuang, S.H., Lee, C.M., Sytwu, H.K., and Wei, F.C. (2018). Blimp-1 prolongs allograft survival without regimen via influencing T cell development in favor of regulatory T cells while suppressing Th1. Mol. Immunol. *99*, 53–65. https://doi.org/10.1016/j.molimm.2018.04.004.

65. Wekerle, T. (2001). Transplantation tolerance induced by mixed chimerism. J. Heart Lung Transplant. *20*, 816–823. https://doi.org/10.1016/s1053-2498(01)00265-0.

66. Sachs, D.H., Kawai, T., and Sykes, M. (2014). Induction of tolerance through mixed chimerism. Cold Spring Harb. Perspect. Med. *4*, a015529. https://doi.org/10.1101/cshperspect.a015529.

67. Yamada, M., Matsuzaka, T., Uetani, M., Hayashi, K., Tsuji, Y., and Nakamura, T. (1995). Normal age-related conversion of bone marrow in the mandible: MR imaging findings. AJR Am. J. Roentgenol. *165*, 1223–1228. https://doi.org/10.2214/ajr.165.5.7572508.

68. Kaneda, T., Minami, M., Ozawa, K., Akimoto, Y., Okada, H., Yamamoto, H., Suzuki, H., and Sasaki, Y. (1996). Magnetic resonance appearance of bone marrow in the mandible at different ages. Oral Surg. Oral Med. Oral Pathol. Oral Radiol. Endod. *82*, 229–233. https://doi.org/10.1016/s1079-2104(96)80262-9.

69. Kulahci, Y., Klimczak, A., Madajka, M., Altuntas, S., and Siemionow, M. (2010). Long-term survival of composite hemiface/mandible/tongue allografts correlates with multilineage chimerism development in the lymphoid and myeloid compartments of recipients. Transplantation *90*, 843–852. https://doi.org/10.1097/TP.0b013e3181f28bb0.

70. Pepini, T., Pulichino, A.M., Carsillo, T., Carlson, A.L., Sari-Sarraf, F., Ramsauer, K., Debasitis, J.C., Maruggi, G., Otten, G.R., Geall, A.J., et al. (2017). Induction of an IFN-mediated antiviral response by a self-amplifying RNA vaccine: implications for vaccine design. J. Immunol. *198*, 4012–4024. https://doi.org/10.4049/jimmunol.1601877.

71. Geall, A.J., Verma, A., Otten, G.R., Shaw, C.A., Hekele, A., Banerjee, K., Cu, Y., Beard, C.W., Brito, L.A., Krucker, T., et al. (2012). Nonviral delivery of self-amplifying RNA vaccines. Proc. Natl. Acad. Sci. USA *109*, 14604–14609. https://doi.org/10.1073/pnas.1209367109.

72. Magini, D., Giovani, C., Mangiavacchi, S., Maccari, S., Cecchi, R., Ulmer, J.B., De Gregorio, E., Geall, A.J., Brazzoli, M., and Bertholet, S. (2016). Self-Amplifying mRNA vaccines expressing multiple conserved influenza antigens confer protection against homologous and heterosubtypic viral challenge. PLoS One *11*, e0161193. https://doi.org/10.1371/journal.pone.0161193.

73. Wu, J., Lizarzaburu, M.E., Kurth, M.J., Liu, L., Wege, H., Zern, M.A., and Nantz, M.H. (2001). Cationic lipid polymerization as a novel approach for constructing new DNA delivery agents. Bioconjug. Chem. *12*, 251–257. https://doi.org/10.1021/bc000097e.

74. Aberle, A.M., Tablin, F., Zhu, J., Walker, N.J., Gruenert, D.C., and Nantz, M.H. (1998). A novel tetraester construct that reduces cationic lipid-associated cytotoxicity. Implications for the onset of cytotoxicity. Biochemistry *37*, 6533–6540. https://doi.org/10.1021/bi9801154.

75. Wolff, J.A., Malone, R.W., Williams, P., Chong, W., Acsadi, G., Jani, A., and Felgner, P.L. (1990). Direct gene transfer into mouse muscle in vivo. Science *247*, 1465–1468. https://doi.org/10.1126/science.1690918.

76. Jirikowski, G.F., Sanna, P.P., Maciejewski-Lenoir, D., and Bloom, F.E. (1992). Reversal of diabetes insipidus in Brattleboro rats: intrahypothalamic injection of vasopressin mRNA. Science *255*, 996–998. https://doi.org/10.1126/science.1546298.

77. Lin, C.H., Wang, Y.L., Anggelia, M.R., Chuang, W.Y., Cheng, H.Y., Mao, Q., Zelken, J.A., Lin, C.H., Zheng, X.X., Lee, W.P.A., and Brandacher, G. (2016). Combined anti-CD154/CTLA4Ig costimulation blockade-based therapy induces donor-specific tolerance to vascularized osteomyocutaneous allografts. Am. J. Transplant. *16*, 2030–2041. https://doi.org/10.1111/ajt.13694.

78. Lin, C.H., Anggelia, M.R., Cheng, H.Y., Wang, A.Y.L., Chuang, W.Y., Lin, C.H., Lee, W.P.A., Wei, F.C., and Brandacher, G. (2021). The intragraft vascularized bone marrow component plays a critical role in tolerance induction after reconstructive transplantation. Cell. Mol. Immunol. *18*, 363–373. https://doi.org/10.1038/s41423-019-0325-y.

79. Oura, T., Hotta, K., Cosimi, A.B., and Kawai, T. (2015). Transient mixed chimerism for allograft tolerance. Chimerism *6*, 21–26. https://doi.org/10.1080/19381956.2015.1111975.

80. Hotta, K., Aoyama, A., Oura, T., Yamada, Y., Tonsho, M., Huh, K.H., Kawai, K., Schoenfeld, D., Allan, J.S., Madsen, J.C., et al. (2016). Induced regulatory T cells in allograft tolerance via transient mixed chimerism. JCI Insight *1*, e86419. https://doi.org/10.1172/jci.insight.86419.

81. Kawai, T., Cosimi, A.B., Spitzer, T.R., Tolkoff-Rubin, N., Suthanthiran, M., Saidman, S.L., Shaffer, J., Preffer, F.I., Ding, R., Sharma, V., et al. (2008). HLA-mismatched renal transplantation without maintenance immunosuppression. N. Engl. J. Med. *358*, 353–361. https://doi.org/10.1056/NEJMoa071074.

82. Demirkiran, A., Bosma, B.M., Kok, A., Baan, C.C., Metselaar, H.J., Ijzermans, J.N.M., Tilanus, H.W., Kwekkeboom, J., and van der Laan, L.J.W. (2007). Allosuppressive donor CD4+CD25+ regulatory T cells detach from the graft and circulate in recipients after liver transplantation. J. Immunol. *178*, 6066–6072. https://doi.org/10.4049/jimmunol.178.10.6066.

83. Ganguly, S., Ross, D.B., Panoskaltsis-Mortari, A., Kanakry, C.G., Blazar, B.R., Levy, R.B., and Luznik, L. (2014). Donor CD4+ Foxp3+ regulatory T cells are necessary for posttransplantation cyclophosphamide-mediated protection against GVHD in mice. Blood *124*, 2131–2141. https://doi.org/10.1182/blood-2013-10-525873.

84. Sucher, R., Lin, C.H., Zanoun, R., Atsina, K.K., Weinstock, M., Pulikkotil, B., Schneeberger, S., Zheng, X.X., Pratschke, J., Lee, W.P.A., and Brandacher, G. (2010). Mouse hind limb transplantation: a new composite tissue allotransplantation model using nonsuture supermicrosurgery. Transplantation *90*, 1374–1380. https://doi.org/10.1097/TP.0b013e3181ff4fc3.

85. Lin, C.H., Sucher, R., Shih, Y.C., Ng, T.W., Mao, Q., Lin, C.H., Lee, W.P.A., and Brandacher, G. (2014). The neck as a preferred recipient site for vascularized composite allotransplantation in the mouse. Plast. Reconstr. Surg. *133*, 133e–141e. https://doi.org/10.1097/01.prs.0000437229.69811.3a.